Project Number: LDA-1205

Spalling Predictions and Associated Capacity Losses from Hydrothermal Effects

Submitted to the Faculty
Of the
WORCESTER POLYTECHNIC INSTITUTE
In partial fulfillment of the requirements for the
Degree of Bachelor of Science
By

Danielle Antonellis

Richard Gala

Friday, March 2, 2011

Approved by:

Professor Leonard D. Albano, Major Advisor

Professor Brian J. Meacham, Advisor

Abstract

Our project investigated fire-induced spalling and the associated losses of cross-section caused by increased pore pressures at elevated temperatures. This was modeled conceptually to explore the impacts of construction and design practices and to analytically evaluate the impacts of cross-sectional losses. The model was tested with normal and high strength concrete column designs consistent with provisions of ACI 318; the fire conditions were based on ASTM E-119. Similar data sets could be considered to further our understanding of fire-induced spalling.

Authorship

This report was authorized by the following individuals, each had specific authorship responsibilities and each collaborated between disciplines across the completion of the project.

Danielle Antonellis 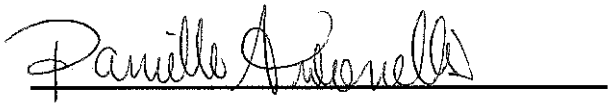

Conducted background research and investigations

Developed conceptual model

Prepared hydrothermal model for testing

Incorporated temperatures based on *ASTM E-119*

Prepared capacity loss model for testing

Executed regression analysis based on published data

Analyzed data results from concrete column capacity losses

Documented work, amended appendices, and acted as the final editor for all chapters

Richard Gala 

Conducted background research and investigations

Developed conceptual model

Designed concrete columns for use in hydrothermal model

Incorporated column mix designs based on *ACI 318*

Prepared capacity loss model for testing

Analyzed data results from concrete column capacity loss tests

Documented work, amended appendices, and acted as the final editor for all chapters

Acknowledgements

Our Major Qualifying Project team would like to thank our advisors, Professor Leonard Albano and Brian Meacham for their help and guidance in completing the project.

Capstone Design

A capstone design experience statement is required for the Major Qualifying Project to highlight the real-world constraints of the project. This MQP was focused on the development and evaluation of a model for spall and its effects, and investigation of design implications. The particular knowledge needed to accomplish this design and analysis came from courses such as Mechanics and Strengths of Materials, Heat Transfer, and Reinforced Concrete Design. This project realistically addressed the economic, sustainability, environmental, health and safety, ethical, and constructability considerations through the design testing, and analyzing processes.

Economic, Sustainability, Environmental

Spalling can cause serious structural damage, sometimes contributing to structural collapse. The property losses associated with spalling have negative effects on the economy, sustainability, and environment. Repairs/reconstruction involves materials, time, and energy which can be very costly. The excess materials and energy used to reconstruct a structure demonstrates unsustainability and has a negative impact on the environment. This MQP includes the development and application of a model for spall and concrete capacity; a full understanding of spalling and its effects is essential to avoid spalling and mitigate its effects.

Health and Safety

This MQP included the development of column designs consistent with provisions of *ACI 318* and fire safety implications associated with the *ASTM E-119* curve, and the discussion of spalling.

Ethics

We complied with the NSPE (National Society of Professional Engineers) Code of Ethics throughout this project. The column designs were based on the most recent code provisions of *ACI 318* and the *ASTM E-119* standard fire curve. The columns were designed with the safety, health, and welfare of the public as our highest priority.

Constructability

The parameters of the model are based on the design and construction phase of reinforced concrete members. The model is meant to give structural designers insight to spalling and its effects and offer practical methods to avoid/mitigate spalling.

Table of Contents

List of Figures

List of Tables

1 Introduction

Every structural designer's intent is to create a structure which will remain stable under expected loads over the life of the building. Designers must consider rare loading conditions, such as seismic, snow, and fire loads in the design phase; a factor of safety is applied to account for construction errors and possible loading conditions as well. Although codes such as the *International Building Codes* [1] and *Eurocodes* [2] require fire resistance ratings on specific members and assemblies, they do not account for all hazards associated with fire environments. Structures, in this case reinforced concrete, may encounter a fire scenario which drastically depreciates the member's ability to withstand customary loading conditions.

There are several mechanisms to be investigated concerning a concrete failure in a fire environment. Spalling is known to be a violent breaking away of concrete which jeopardizes the ultimate capacity of a member. During a fire scenario, increased temperatures at the surface of the concrete can affect the makeup and materials of the specimen – the changes near the surface can result in a spall that not only reduces the area of the column section, but can also expose the reinforcing steel. Given the importance of a spall to the structural integrity during fire conditions, there is limited ability to predict a spall.

Advancements in building construction over the last few decades have delivered structures which were once unimaginable. Demand for taller and more ornate structures requires the addition of stronger concrete systems to compensate for the added loading. Concrete strengths and materials have gradually improved over the years to compensate for these structural fluctuations. The increases in strength have further complicated the problem of spalling in concrete members. Key parameters of the spalling issue include the concrete mix design, material interactions various materials and actions of concrete during a fire scenario.

It is imperative to investigate the design of concrete members and how they react in a fire environment. Accessible data shows relationships between concrete's aggregates, strengths, admixtures, and pore pressure. Through examination of the spalling mechanism, pore pressure was selected as the most important aspect to the spalling phenomena. Previous research on pore pressure as it pertains to spalling has been done, but only in terms of high strength concrete which is assumed to spall worse than normal strength concrete [3]. High strength concrete and normal strength concrete differ in their mix designs by the amount of water added and certain

admixtures included in high strength concrete that are excluded in normal strength concrete. The purpose of this study was to explore spalling of normal strength concrete and high strength concrete members of similar mix matrix to quantify the differences of performance under thermal conditions.

This study identified relevant experimental data and related it to the current analytical procedures and code regulations to design normal strength and high strength reinforced concrete columns. These columns posed as facilitators to determine the propensity of concrete to spall. This model was based on the hydrothermal behavior of concrete at elevated temperatures, as described by Kodur [3], who has performed research on fire-induced concrete spalling and claims pore pressure is the most influential factor. The importance of water vapor in the context of pore pressure and spalling will be discussed in further detail. This investigation also included calculations on capacity losses of concrete at elevated temperatures to give structural designers insight to the effects of spalling. Data from several sources was used to quantify the effects of spalling on normal strength concrete and high strength concrete members, allowing comparisons between the different types of concrete.

2 Background

2.1 Concrete Design and Construction

The design and construction of reinforced concrete structures greatly influences the concrete's propensity to spall. Much consideration goes into a design because it must adhere to a variety of codes and specifications. The various aspects of concrete design and construction include the concrete's mix design, the quality of construction, type of reinforcement, amount of cover protection, and its geometry. Each of these aspects and their relationship to spalling are explained below. An investigation of these factors and their contribution to spalling have allowed for assumptions to be made for this particular model to be created.

2.1.1 Concrete Mix Design

Concrete can be classified into two categories Normal Strength Concrete (NSC) and High Strength Concrete (HSC). NSC has compressive strength below 35MPa (5000 psi), whereas HSC has compressive strength above 35MPa. Concrete strength is a function of its concrete mix design. The fundamental ingredients of concrete (cement, aggregate, water, and admixtures) are similar between mixes but the properties of the specific materials and their quantities vary mix-to-mix. The quantity and type of these materials make up the major differences between concrete classifications.

The cementious material used in a concrete mix is known as Portland cement. According to the Portland Cement Association the cement paste is…

> "…composed of Portland cement and water, coats the surface of the fine and coarse aggregates. Through a chemical reaction called hydration, the paste hardens and gains strength to form the rock-like mass known as concrete [4]."

The American Society for Testing and Materials (ASTM) C 150 identifies and describes ten types of cement, shown in Figure 1. Properties of these cements vary- including air-entrainment, sulfate resistance, or strength. The designer chooses the type of cement to use based on the necessary concrete properties for the specified application. Each cement reacts differently during hydration, therefore each type has a different potential to spall. The type and amount of cement

contributes to the concrete's strength which plays a major role in determining if the concrete is prone to spalling.

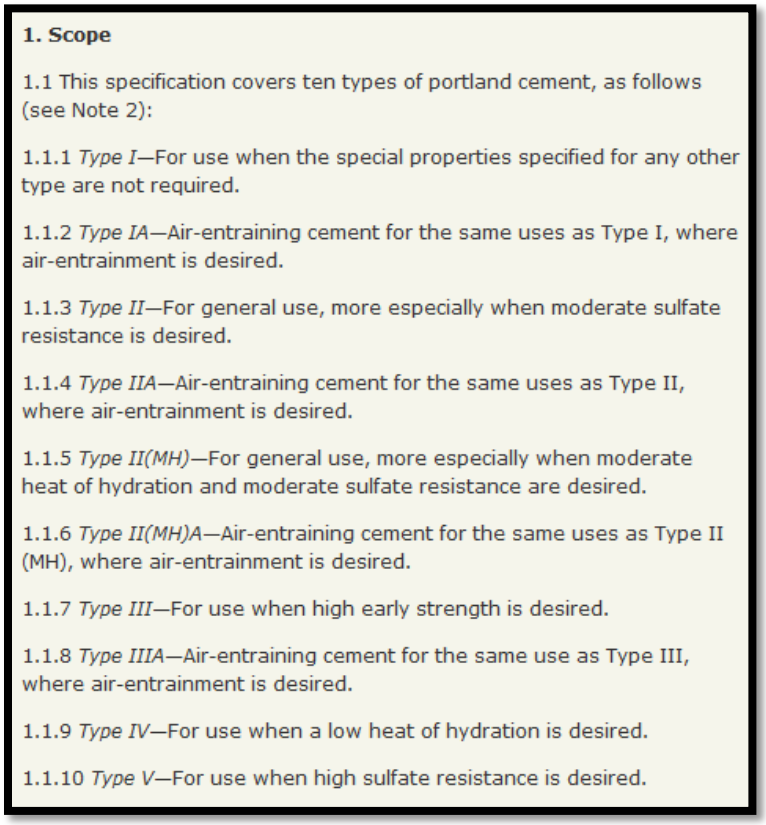

1. Scope

1.1 This specification covers ten types of portland cement, as follows (see Note 2):

1.1.1 *Type I*—For use when the special properties specified for any other type are not required.

1.1.2 *Type IA*—Air-entraining cement for the same uses as Type I, where air-entrainment is desired.

1.1.3 *Type II*—For general use, more especially when moderate sulfate resistance is desired.

1.1.4 *Type IIA*—Air-entraining cement for the same uses as Type II, where air-entrainment is desired.

1.1.5 *Type II(MH)*—For general use, more especially when moderate heat of hydration and moderate sulfate resistance are desired.

1.1.6 *Type II(MH)A*—Air-entraining cement for the same uses as Type II (MH), where air-entrainment is desired.

1.1.7 *Type III*—For use when high early strength is desired.

1.1.8 *Type IIIA*—Air-entraining cement for the same use as Type III, where air-entrainment is desired.

1.1.9 *Type IV*—For use when a low heat of hydration is desired.

1.1.10 *Type V*—For use when high sulfate resistance is desired.

Figure 1: Standard Specification for Portland Cement [5]

The cement is mixed with water to create cement paste; the proportion of water to cement is called the Water-to-Cement Ratio (W/C). Extreme heated curing environments can cause physical and chemical changes in the cement paste, which can also affect the aggregate involved. It is possible the overall structure could be weakened because of a loss of strength in the cement paste [6]. If the concrete were to weaken prior to being fully loaded or placed in an environment, the concrete is even more prone to failure.

Higher W/C increases the workability of the concrete, or ease of placement, but excess water may have a negative impact on the quality of the concrete. Excess water can cause segregation of the aggregate components from the cement paste. The excess water may be released from the concrete as it hydrates because the concrete is already saturated. This result may produce weak, brittle concrete which is insufficient for the original concrete design.

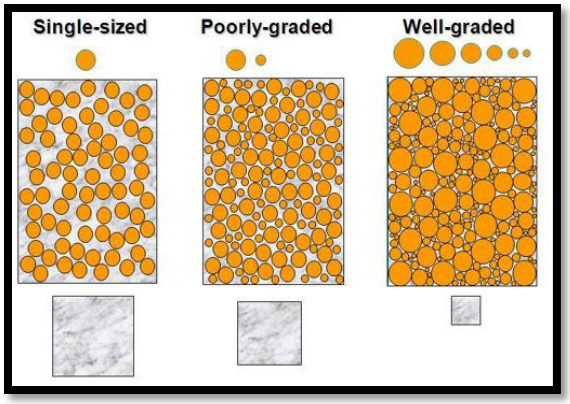

Figure 2: A Comparison of Void Space with Different Aggregate Gradations [7]

Aggregate is another essential ingredient of concrete. There are numerous types of aggregate, ranging in shape, size, strength, and more. Type of aggregate has a large influence on the overall strength of concrete. Aggregate occupies approximately 60-80 percent by volume of the concrete. Gravel, crushed rock, or limestone is typically used as aggregate; the type is often limited by geographical availability [8]. The concrete mix design specifies the amount and distribution of aggregate sizes (coarse and fine) which are directly proportional to the void space in cured concrete. This void space is related to the porosity of concrete; Figure 2 shows the aggregate of three different grades of concrete. Concretes with high porosity have high permeability which correlates to less buildup of pore pressure and thus less explosive spalling. The thermal strain and thermal conductivity of concrete are also controlled by the type of aggregate; certain physic-chemical changes may occur in the aggregate as well, therefore aggregate has a large influence on concrete's performance at elevated temperatures.

This paper will focus on carbonate and siliceous aggregates, which are to be associated with explosive spalling [9]. Carbonate aggregate (predominantly limestone) provides a higher fire resistance and better spalling resistance than siliceous aggregate (predominantly quartz) [10]. Carbonate aggregate has higher strength than siliceous aggregate because it is more of a heavy weight specimen.

The last component of a concrete mix is the admixtures, typically chemical. According to PCA [4], admixtures are used to reduce the cost of concrete, to modify some of the properties of hardened or cured concrete, to ensure utmost quality of concrete during the mixing, transporting, placing, and curing processes; and to overcome any emergencies which may occur during concrete operations. Admixtures are classified by their function; PCA defines five main

functions: water-reducing admixture, retarding admixtures, accelerating admixtures, superplasticizers, and corrosion-inhibiting admixtures. Water-reducing admixtures reduce the required W/C but maintain high workability. The retarding admixtures slow the setting rate of the concrete and are used to counteract the accelerating effect of hot weather and temperatures on the concrete during setting. An accelerating admixture is used to increase the development of early strength, reduce the time to protect and cure the concrete, and speed up any other finishing operations. Those types of admixtures are usually used in cold weather settings. Superplasticizers are used to reduce the water content of concrete by twelve to thirty percent. This is usually used to take a concrete which has a low-to-normal slump and change it into a high-slump flowing concrete which can be placed with little or no compaction or vibration. Strength admixtures such as silica fume are often added to concrete mixes to increase the strength of the cement paste and its bond to the aggregate. Silica fume produces calcium silicate hydrates (CSH) when mixed with Portland cement and water- this CSH "gel" (gel water) is responsible for the added strength [11].Lastly, corrosion-inhibiting admixtures are used to slow the corrosion of the reinforcing steel in the concrete for conditions exposed to higher levels of chloride [4]. Concretes exposed to the outside environment typically need these admixtures.

All of these admixtures have the ability to decrease permeability, improve durability, inhibit corrosion, reduce shrinkage, and increase the workability of the concrete [12]. Each admixture has specific applications and processes for installation; if used appropriately admixtures may help reduce the risk of spalling. However, admixtures can also have a negative impact on concrete's propensity to spall. For example, Silica Fume is added to some HSC which reduces permeability; as discussed concretes with lower permeability are more prone to spalling [13].

Figure 3: Ingredients of Concrete [14]

The concrete mix design involves many factors and a simple design or mixing error could lead to a catastrophic disaster. An error in the type of cement or aggregate used will dramatically alter the concrete's durability and strength and could lead to a failure when loaded or entered into a heated environment. The concrete mix design will be a large aspect of this study when considering the heating environment that it may encounter in a fire scenario.

2.1.2 Construction Quality

Figure 4: Pouring and Curing Concrete [15]

Concrete mix designs are defined in construction specifications, but the quality of the installation is not in the designer's control. The contractor is responsible for accepting/declining the concrete delivered to the site, proper placement and the curing techniques as specified in The American Concrete Institute's *ACI 318: Building Code Requirements for Structural Concrete*. If the contractor does a poor job, the concrete quality will suffer. Although it is the contractor's professional responsibility to adhere to the mix design, contractors can be tempted by better economics to add extra water to the mix, for example. Extra water decreases the proportions of cement and increases workability, thus it decreases the labor costs. However, increasing the W/C has significant negative impacts on the concrete strength. Practicing good construction quality methods such as having good mixing conditions, good curing conditions, using air-entrainment, and compaction and vibration, will contribute to a strong concrete over its lifetime. Concrete with insufficient construction quality may not be able to handle the applied loads and could result in a failure, even spalling.

The temperature of the environment at the time of placement has a large impact on curing. Severe cold or hot weather environments may greatly affect the speed at which the concrete cures and can affect the early and permanent strength of the concrete. At colder temperatures, concrete gains strength significantly slower than when cured at higher temperatures. Concretes in environments below 40ºF will reach thirty-five percent of its design strength by the seventh day of curing [16]. This is not optimal for concrete reaching its peak strength and could result in a decrease in overall concrete strength. Shrinkage cracks may occur at higher temperatures when the rate of evaporation of the water is greater than the production of bleed water in the concrete. Bleed water is released from the surface of the concrete because it has the lowest specific gravity among all the materials in the mix; bleed water occurs in mixes with excess water [17].

Carbonation of concrete is a process in which carbon dioxide combines with the hydration products of Portland cement to create calcium carbonate [18]. This byproduct, calcium carbonate, is a known acid which has the ability to degrade cement. If the acid were to degrade the cement compounds it could weaken the bonds between the aggregates and severely weaken the strength and durability of the concrete. This makes the concrete prone to spalling when it is placed into a heated environment.

Air-entrainment, or the air content of the concrete, has been used to protect the concrete during its curing process. The process for air-entraining was developed in the late 1930s, and is now recommended for concrete's subject to freezing and thawing cycles [4]. Freeze-thaw can severely affect the concrete's properties during the time in which it is curing. Air-entrainment improves resistance to freezing by creating billions of microscopic air cells which relieve internal pressure on the concrete by providing tiny chambers for the expansion of water when it freezes [4]. To air-entrain a concrete mix you must introduce the air-entraining admixtures during the mixing of the concrete on the job site. Since this admixture protects the concrete from any severe freeze-thaw issues, it can also protect it from losing any of its strength and durability throughout its lifetime. Air-entrainment can reduce concrete's propensity to spall because the air voids will relieve the vapor pressure. The concrete design used for this study will be exposed to an interior environment and thus will not need air-entraining.

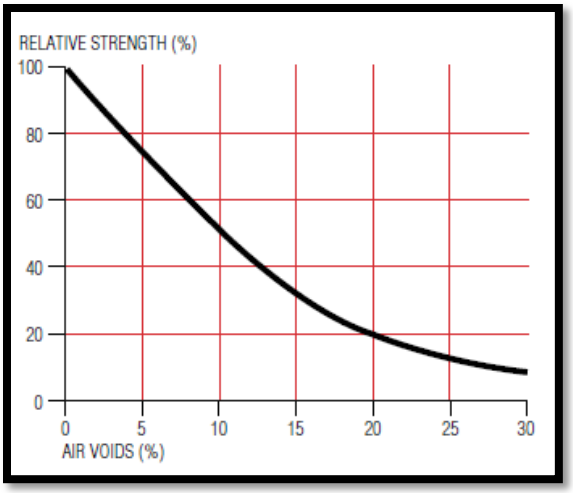

Figure 5: Loss of Strength through Incomplete Compaction [19]

Compaction expels entrapped air from freshly placed concrete and packs the aggregate close together to increase the concrete's overall density and reduce porosity. Compaction decreases the number of air voids, which increases the strength of the concrete; see Figure 5. This results in a significant increase in the ultimate strength, an enhanced bond with the reinforcement, an increase in abrasion resistance, and an increase in durability [19].

Vibration allows concrete to release entrapped air. The vibration of concrete can improve its compressive strength by approximately 3-5 percent for each percent of air removed. The amount of time a concrete mix should be vibrated depends on the slump (or W/C) of the sample. Mixes with higher W/C should be vibrated for a longer duration to ensure a higher compressive strength [20].

The contractor should vibrate and compact concrete to obtain the highest ultimate strength. Higher strength will allow the concrete to take on greater loading conditions, but higher strength concrete is more prone to explosive spalling. This phenomenon is well accepted in the research community and will be explained in further detail later.

Overall, there are various methods to maintain a safe and acceptable construction quality. Proper mixing conditions, curing conditions, air-entrainment, compaction, and vibration of concrete help it gain strength and durability during placement and curing. This is essential when concrete is placed in for use in an environment with increased loading and possibly the high temperature conditions associated with fire. These methods should be used to ensure the concrete is sufficiently stable prior to being placed in any type of environment. It is essential to ensure that the concrete contractor is acting properly and is placing and mixing the concrete as designed

and specified. Although sometimes overlooked, construction quality is a part of every job and required by building codes. The numerous variables and scope of construction quality activities results in a complex thermodynamic history for the concrete.

2.1.3 Reinforcement

Figure 6: Deformed Reinforcing Steel [21]

Concrete is strong in compression but weak in tension. Improving the tensile strength of concrete makes it more stable and allows for the member to take on greater loads. The objective of reinforcing steel is to increase the tensile strength of a member. Reinforcements of all types (steel, mesh, or fibers) are used in most concrete construction, including reinforced concrete and prestressed concrete. According to the American Concrete Institute (ACI) there are a variety of reinforcements ranging from plain steel bars, deformed steel bars, cold-drawn wire, welded wire fabric, deformed welded wire fabric, and fibers [22]. Deformed steel bars are round steel bars with lugs rolled into the surface of the bar during manufacturing which create a mechanical bond between the concrete and the steel when set in place. These bars come in eleven different sizes and thicknesses to account for the differing sizes of structural concrete members and components which require a greater amount of tensile strength [21]. Welded wire fabric reinforcement is a square or rectangular mesh of wires welded at all intersections which helps to prevent shrinkage cracks in slabs by resisting severe temperature change. The most common use for wire mesh in columns is as tie reinforcements. Minimizing shrinkage cracks in a column cross-section will minimize the loss of strength and ability for the section to spall. Fiber-reinforced polymer bars has been shown to mitigate the effects of spalling. Spalling can be caused by corrosion, not just

at elevated temperatures, therefore fiber-reinforced bars should be used in areas where the corrosion of a regular deformed steel bar is likely. Fiber-reinforced polymers thermally expand and contract at a rate close to that of the concrete, they do not rust, and they have a very high strength-weight ratio- all properties that prevent spalling [22]. These fibers also respond well to elevated temperatures.

Placement of reinforcing bars is just as important as the type and size. Improper placement of steel can result in a severe loss in strength, especially in tension. Some parameters which should be checked before placing steel are the concrete cover, the flexural design theory, the lap length, the development length, and the bar spacing and size. If the steel is placed with less concrete cover than is necessary, the life of the reinforcing steel can be shortened due to failure factors such as corrosion [22]. When looking at the flexural design theory the neutral axis of the concrete is considered. The neutral axis is the area of the concrete neither in compression or tension because it is at the point at which the stress changes from one to the other. According to this theory, the steel reinforcements must be placed in such a manner to maintain its tensile strength and support the concrete:

> "When the section flexes downward the concrete and reinforcing steel above the neutral axis are in compression and at the same time, the concrete and reinforcing steel below the neutral axis are in tension. As the section below the neutral axis is stretched by the tensile force, the steel and concrete stretch together at the same rate due to the bond between the reinforcing steel and concrete. During this stretching, the reinforcing steel elongates and retains its tensile strength." [23]

Placing steel above and below the neutral axis of the concrete allows the concrete to gain strength and maintain its durability.

Another aspect of steel reinforcements is their lap length. Lap length is the minimum length required to transfer stress from one bar to another because steel reinforcements do not have extremely long ranges [24]. Determining the lap length will also help to determine the number of bars needed over a particular span. Once the total number of bars is determined the previous techniques can be used to determine adequate placement. Proper placement of the steel reinforcement, no matter what type it is, is essential to lessen the chance of spalling occurring in a column.

2.1.4 Concrete Cover

The concrete cover is the amount of concrete which is used to cover and protect the steel reinforcements within the column. The cover protects the steel reinforcements from corroding due to any environmental issues they may encounter, as well as slipping and debonding. In terms of this study, it is important to note that concrete cover also contributes to the fire resistance of the section by insulating the steel. *ACI 318* defines the amount of concrete cover required to protect reinforcement. According to ACI, a 3" and 1.5" minimum concrete should be used to protect concrete that is permanently exposed to earth and subject to interior conditions respectively. The amount of cover directly depends on the concrete application and type of environmental exposure (see Figure 7). The term "minimum concrete cover" is used by the ACI committees and should be recognized by the contractors when placing the concrete over the reinforcements [25]. Contractors will not typically install additional concrete cover because of added cost. The amount of concrete cover is important when considering the degree of spalling. Large losses of cross-section may result with the reinforcing steel being exposed, which would result in large capacity losses.

CODE

7.7 — Concrete protection for reinforcement

7.7.1 — Cast-in-place concrete (nonprestressed)

The following minimum concrete cover shall be provided for reinforcement, but shall not be less than required by 7.7.5 and 7.7.7:

	Minimum cover, in.
(a) Concrete cast against and permanently exposed to earth	3
(b) Concrete exposed to earth or weather:	
No. 6 through No. 18 bars	2
No. 5 bar, W31 or D31 wire, and smaller	1-1/2
(c) Concrete not exposed to weather or in contact with ground:	
Slabs, walls, joists:	
No. 14 and No. 18 bars	1-1/2
No. 11 bar and smaller	3/4
Beams, columns:	
Primary reinforcement, ties, stirrups, spirals	1-1/2
Shells, folded plate members:	
No. 6 bar and larger	3/4
No. 5 bar, W31 or D31 wire, and smaller	1/2

Figure 7: Minimum Concrete Cover for Cast-in-place (Non-Prestressed) Concrete [25]

2.1.5 Geometry

Column geometry is typically specified by the architect, and is often based on the load requirements and aesthetics of the column. The three most common column geometries will be considered in this section: square, rectangular, and circular columns. Of course, an architect may choose to create a non-traditional column shape, but those are normally precast and prestressed members. These guidelines may be tailored to the non-traditional column shapes to determine if they are at risk for spalling.

The major difference between the ordinary column shapes square and rectangular columns and circular columns is the presence of corners. The eccentricity from the side of a column to the steel reinforcement and from the corner of a column to the steel reinforcement can be calculated from the load and moment diagrams. Nilson [26] describes that a relatively small eccentricity will characterize a rectangular and square column in compression while a larger eccentricity will subject the column to tension over a part of the section. Overloading these columns must be avoided to avoid failure. Eccentricities for a circular column are taken from the steel reinforcements to the outer radius of the column. A smaller eccentricity for a circular column allows the column to show greater toughness and ductility [26]. Of course, all columns are designed with similar concrete mixes and show similar strengths within the same structure. The issue of corner spalling is presented later in this report.

2.2 Spalling in a Fire Environment

Spalling due to increased temperatures is a function of concrete's properties, the fire environment, and the applied stresses. It is essential to understand the interactions of each parameter's impact on a member's ability to resist spalling. The concerns related to the fire environment are the heat transfer to the column and within the column cross-section. These heat transfer values are functions of several factors, including compartment geometry, fuel load, ventilation, location of the fire, and location of the element of concern. Spall is related to the pore pressure increase associated with temperature increase. The following looks at factors affecting temperature increase, resulting in pore pressure increase, and the associated effects on structural strength.

2.2.1 Fire Environment

It is critical to understand the effects of fires on spalling. Parameters such as the peak temperature, heat release rate (HRR), and the location of the heat source give insight to the potential degree of spalling. Most testing data is based on the *ASTM E119* and *ISO 834* temperature-time curves to normalize data, as shown in Figure 8. This testing is done to support the concept of fire resistance ratings, which building codes rely on to define structural fire safety requirements. These standard fire curves normalize data from fire resistance testing; they also enable comparisons to be made between data sets from different experiments since the HRR and peak temperatures are virtually identical.

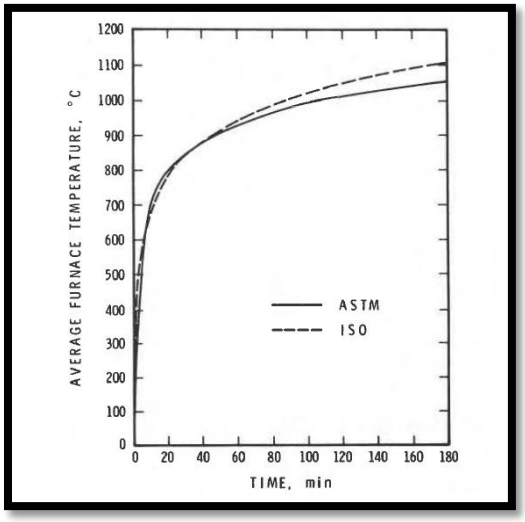

Figure 8: Comparison of *ASTM E119* and *ISO834* temperature-time curves [27]

2.2.1.1 Heat Release Rate

The heat release rate (HRR) describes the rate at which heat is generated in a fire. This rate depends on many parameters- such as the combustible materials in the space (fuel) and the ventilation (oxygen).

2.2.1.2 Peak Temperature

The peak temperature is an important parameter to explore. Material properties are affected at high temperatures- basically every thermal reaction is magnified as the temperature increases. For example, at high temperatures, the microstructure of the cement itself decomposes and releases vapor which increases the vapor pressure and can cause spalling [28].

2.2.1.3 Heat Source

Localized heating burning versus burning throughout the compartment, the magnitude and duration of the fire all need to be considered, with a need to predict the heat transfer to the column over time.

2.2.2 Fire-Induced Stresses

All concrete structure types are subject to stresses, but for this MQP a column will be investigated. Columns are exposed to a variety of stresses, from live and dead loads to corrosion. Some stresses occur over long periods of time, others are caused by the environment, aging, unexpected loading conditions, etc. The magnitude of these stresses and the column's reaction to them will greatly impact the column's propensity to spall. From a design perspective, engineers consider the compressive and tensile stresses that will be applied to a given column. An appropriate concrete mix and steel reinforcement design should mitigate concerns associated with daily loading conditions. The designer's factor of safety should help protect against unexpected conditions, such as creep.

2.2.2.1 Creep

"Creep is the plastic deformation of a material that is subjected to a stress below its yield stress when that material is at a high homologous temperature. Homologous temperature refers to the ratio of a materials temperature to its melting temperature. The homologous temperatures involved in creep processes are greater than 1/3" [29]. Creep is more significant at higher stress levels and elevated temperatures (see Figure 10). Figure 9 is a curve of creep over time; the curve steepens as additional stress or heat is applied to the material.

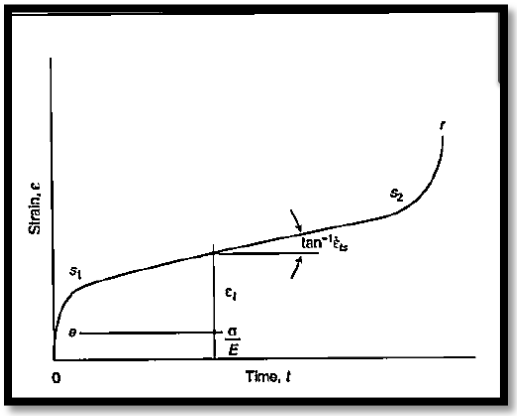

Figure 9: Creep Strain vs. Time Curve (T=constant; σ = constant) [30]

Creep at elevated temperatures is considered "thermal transient creep"; it is due to thermal and hygral gradients in the concrete. For example, if the cement paste experiences deformations, it will cause stress to the aggregate, which will further increase the creep.

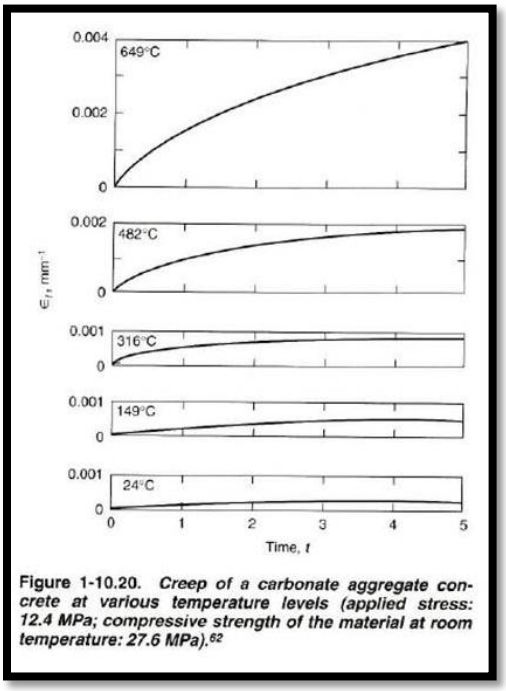

Figure 1-10.20. *Creep of a carbonate aggregate concrete at various temperature levels (applied stress: 12.4 MPa; compressive strength of the material at room temperature: 27.6 MPa).*[62]

Figure 10: Creep of Carbonate Aggregate Concrete at Various Temperatures [30]

2.2.2.2 Pore Pressure

Types of Water

Concrete contains a significant amount of water. During the mixing process, a prescribed amount of water is added to the concrete mix. This water can be found in three different forms- chemically-bound water, gel water, and free water, depending on the status of the hydration process. Chemically-bound water mixes with the Portland cement during hydration to form the paste. Chemically bound water is "driven off" at 105ºC (the phrase "driven off" will be clarified in this section) [31]. Free water is located in the coarse pores of the cement paste. Figure 11 shows how the role of water changes depending on the status of hydration.

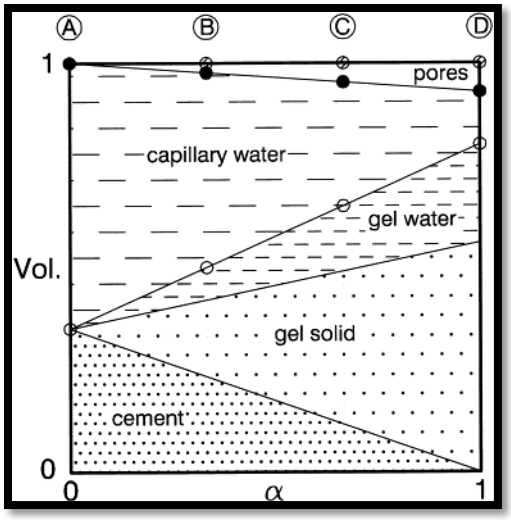

Figure 11: Volumetric Phase Distribution of Cement Paste as a Function of the Degree of Hydration at W/C=0.6 [31]

Water Clog Phenomena

As the temperature of concrete increases, gel water and chemically-bound water are released into the pores through desorption and dehydration, respectively (see Figure 12). Desorption is the process by which the water within the concrete is released from or through its surface [32].

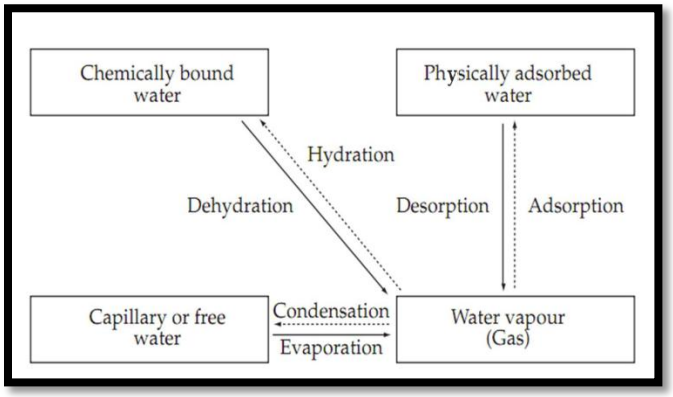

Figure 12: Water Processes in Concrete [33]

The water at the surface is released into the atmosphere. The water in the deeper portions of the concrete migrates inward, toward the cooler portion of the concrete. This migration of water causes the inner pores to become saturated. The water vaporizes at the interface between the dry surface and the saturated inner concrete. The time–temperature curve in shows a plateau in Figure 13 at approximately 150ºC which represents a phase change (vaporizations).

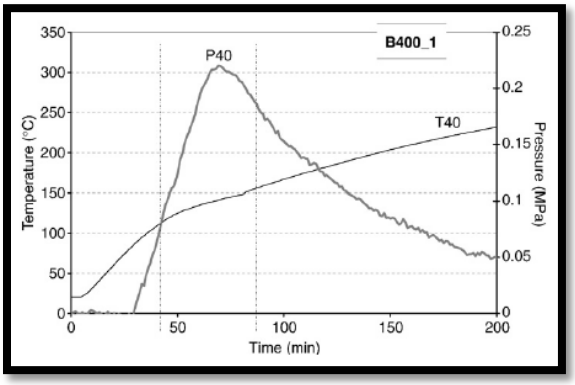

Figure 13: Time-Temperature Curve and Time-Pressure Curve for Concrete [34]

At the same time, the peak pressure is reached. If this pore pressure is greater than the tensile strength of the concrete, a spall will occur. This is known as the "Moisture Clog Phenomena" (shown in Figure 14).

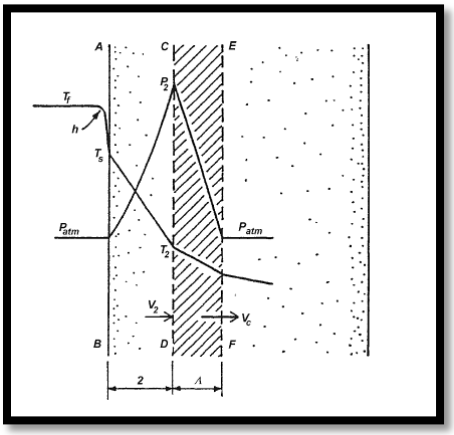

Figure 14: Moisture Clog Phenomena [8]

These water types and actions are directly linked to the pore and vapor pressure buildup in concrete at elevated temperatures. Applying this knowledge with previous work done by Kodur [3] allowed for the proposed model for spall to be created. Within the model pore pressure and porosity will be the focus, and both these concepts deal with the water content of the concrete.

Development of the model is presented in the Methodology and Appendix D. The model will help to predict spalling in terms of pore pressure.

A study of spalling as a possible failure mechanism in fire conditions was conducted. The influences of concrete design and construction, fire environment, and heat related stresses on concrete's propensity to spall have been documented in this section.

3 Methodology

This project began with in depth research on spalling and all factors that contribute to it. Several factors were identified as influential to concrete's propensity to spall; the model described herein was based on the water content's impact on spalling. The amount of water in concrete affects the strength and permeability of the concrete, as well as the pore pressure in a fire environment. This parameter was chosen because designers can change the water-to-cement ratio rather easily compared to the type of aggregate, for example, which has limited choices because of geography (there are large cost increases associated with shipping aggregate). Fire-induced spalling has been attributed to high pore pressures in previous studies, such as Kodur's "Hydrothermal model for predicting fire-induced spalling in concrete structural systems" [3].

Increased temperatures cause the various water types within concrete to transform into their gaseous states, causing pore pressure to increase. The moisture clog phenomenon causes continuous redistribution of moisture during a fire event and creates a constant cycle of vapor conversion, which attributes to the spalling of a cross section. Permeability, a material's ability to allow water to flow through it, is an important factor in the development of concrete pore pressure. Samples with lower permeability have greater buildup of vapors due to the entrapment of the water in the pores. In terms of water content, greater volumes of water present in the concrete will not only reduce its ultimate strength during curing, but also increase the amount of vapor in a fire environment. Controlling these factors could reduce the propensity of a column to spall explosively and thus lose capacity.

To incorporate the concept of pore pressure into an analytical model, all of the components of concrete design and strength had to be considered. To help display pore pressure's influence on spalling, the concrete's water-to-cement ratio (W/C) and permeability were the two most important values investigated. Available data from research done by Kodur [3] has allowed for the determination of a concrete's temperature and pore pressure at various depths. By correlating this information with the tensile strength and porosity of the concrete (derived from the W/C [35]), the conditions at which a spall will occur can be identified. The analytical model in this section will show how to predict spalling as a function of pore pressure and how to calculate the capacity losses of a reinforced concrete member. Results from this model give insight to the propensity of a member to spall and the associated impacts.

Figure 15 is a flow chart that guides the reader through the basic steps of the model's methodology. Essentially, the model determines what conditions are necessary for a spall to occur and the capacity losses associated with specified degrees of spalling.

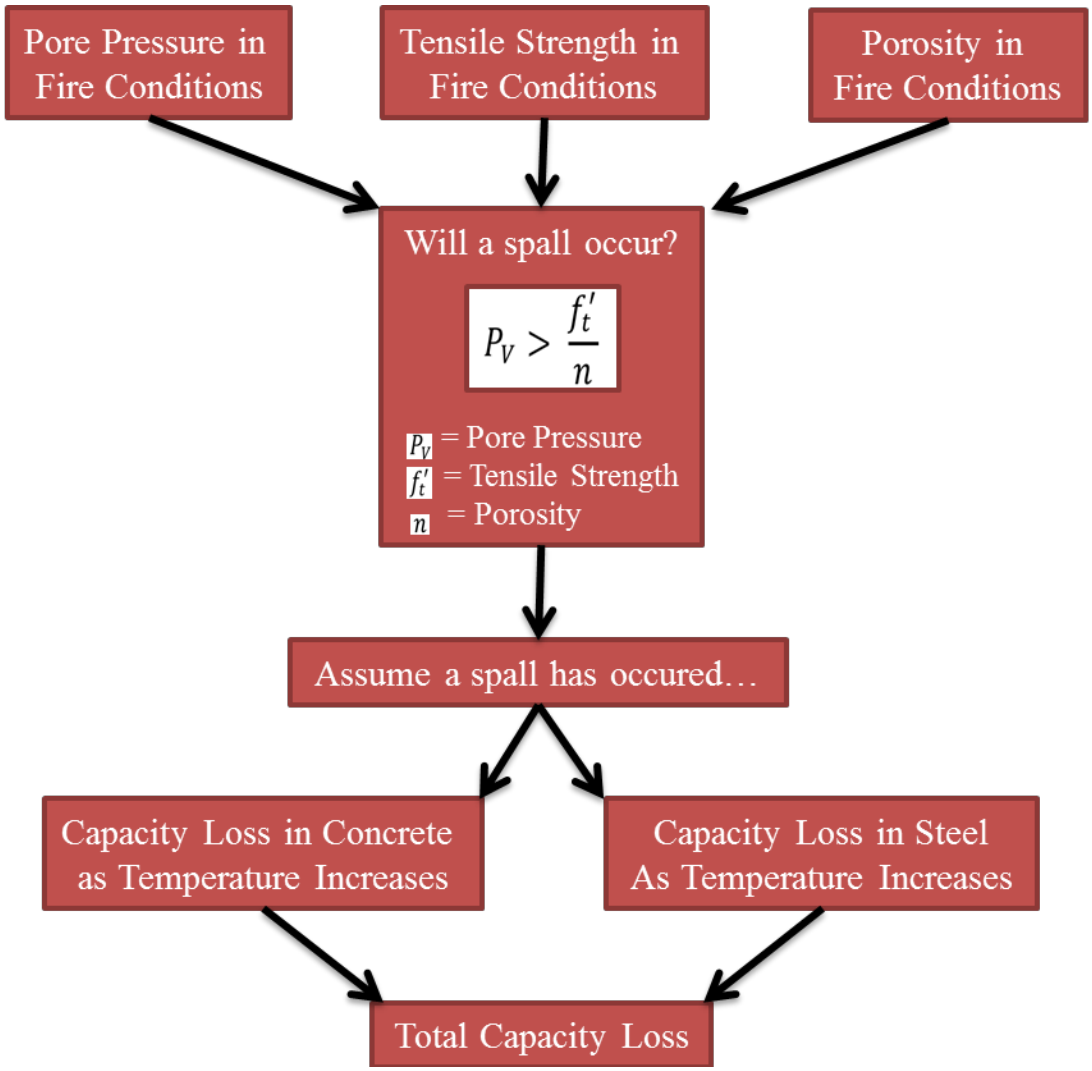

Figure 15: Methodology Flow Chart

This is a conceptual model; we identified factors that need to be considered. At present, no single document, standard, or guide provides data for all aspects considered at elevated temperatures. We used various sources for the needed data. In particular, we used the *ASTM E-119* curve to reflect the fire environment and temperatures within concrete. We used *Eurocode 2* [2] and the "Structural Fire Protection Manual, Manual No. 78" from ASCE [36] to predict the compressive and tensile strengths of concrete at elevated temperatures, respectively. To

determine the compressive strength of concrete at elevated temperatures data was used which correlated to the work of Bastami [37] who interpolated graphical data issued in *Eurocode 2* and Chapter two of *ASCE Manual No*. 78. The predictive equations provided by Bastami [37] were used for this analysis. The yield strength of the steel and the porosity of the concrete were based on experimental data. We calculated column capacity based on an equation presented in *ACI 318*.

3.1 Propensity to Spall

The analytical model presented in this report is reproducible if certain data sets are available. Pore pressures at specified depths from the exposed surface, as a function of temperature and the associated time-temperature curves are necessary.

This report used Kodur's "Hydrothermal model for predicting fire-induced spalling in concrete structural systems" [3] which predicts spalling of concrete structures based on pore pressure as a function of time to perform analysis. This publication provides model test data validations against experimental data in graphical form. These validations include "Time versus Temperature" and "Time versus Pore Pressure" curves at various depths of a concrete slab, both based on the *ASTM E119* [38] standard fire curve (see Figure 16 and Figure 17, respectively). The *ASTM E119* standard fire test curve is shown in Figure 18. The "Time versus Pore Pressure" curves illustrate the changes in pore pressure in concretes with permeability coefficients (k) between $2 \times 10^{-18} m^2$ and $20 \times 10^{-18} m^2$ [3]. Non-porous concretes are more susceptible to spalling than concretes with a higher permeability.

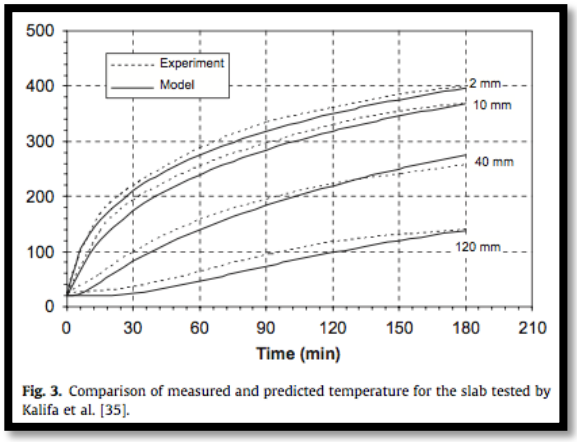

Fig. 3. Comparison of measured and predicted temperature for the slab tested by Kalifa et al. [35].

Figure 16: Time versus Temperature curves at various depths of a concrete slab [3]

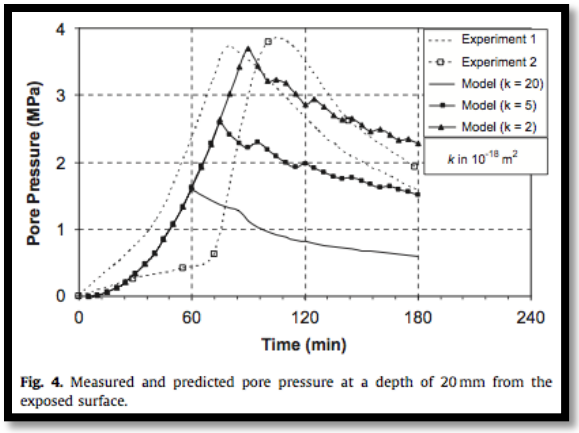

Fig. 4. Measured and predicted pore pressure at a depth of 20 mm from the exposed surface.

Figure 17: Time versus Pore Pressure at a depth of 20mm form the exposed surface [3]

The value "k" in Figure 17 represents the permeability of the concrete specimen. Concrete with low permeability has higher pore pressure because the water vapor cannot escape from the pores. Graphs of "Temperature versus Pore Pressure" were created for concrete at specified depths; the depths used were chosen based what pore pressure and temperature data was available.

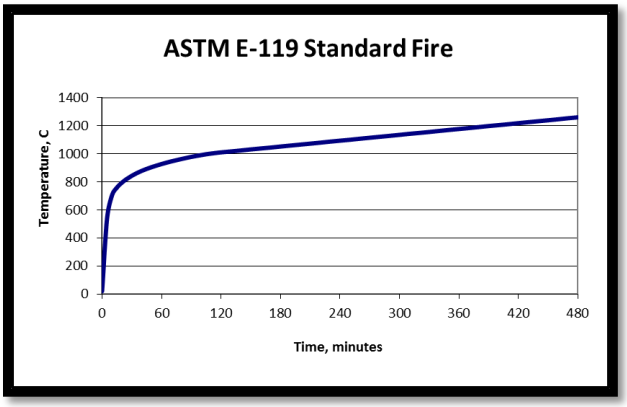

Figure 18: *ASTM E119* Standard Fire Curve [38]

A comparison between the pore pressure values and the tensile strength of concrete was made to quantify the propensity to spall. According to Kodur [3], spalling occurs when pore pressure exceeds the tensile strength of concrete, as demonstrated in Equation 1, where P_V is the pore pressure at the specified depth from the exposed surface, f_t' is the tensile strength of the concrete, and n is the porosity of the concrete. This equation is the fundamental concept that supports the spalling prediction model presented.

Equation 1: Spalling predictor based on pore pressure [3]

$$P_v > \frac{f_t'}{n}$$

It was necessary to determine the tensile strength of concrete as temperature increases. Equation 2 which represents the loss of concrete's tensile strength as temperature increases (f_{tT}').

Equation 2: Tensile strength as a function of temperature [39]

$$f_{tT} = \begin{cases} f_t, & T \leqslant 100\,^{\circ}\mathrm{C} \\ f_t \frac{600-T}{500}, & 100\,^{\circ}\mathrm{C} < T \leqslant 550\,^{\circ}\mathrm{C} \\ f_t \frac{1200-T}{6500}, & 550\,^{\circ}\mathrm{C} < T \leqslant 1200\,^{\circ}\mathrm{C} \\ 0, & T > 1200\,^{\circ}\mathrm{C} \end{cases}$$

The porosity does not vary over temperature but it does depend on the concrete mix. The porosity of the concrete was based on Hernandez's "Porosity Estimation of Concrete by Ultrasonic NDE" [35] which gave the porosity of concrete as a function of its water-to-cement ratio (W/C).

3.2 Capacity Losses Associated with Spalling

Fire-induced spalling has the potential to significantly reduce a concrete member's cross-section and, in turn, drastically affect its maximum allowable capacity. Figure 19 is a simplified illustration of the potential cross-section losses a reinforced concrete column may experience due to spalling. This figure illustrates various degrees of spalling, ranging from no spalling to spalling equivalent to the complete loss of concrete cover, thus exposing the reinforcing steel.

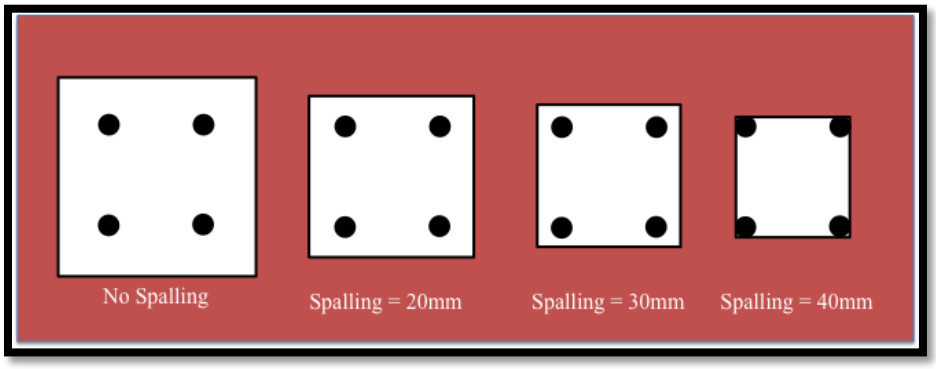

Figure 19: Cross-section losses associated with spalling

The capacity of the reinforced concrete members were determined to monitor the strength losses as the temperature increased. Refer to Appendix B for the column capacity equation from ACI-318 equation 10-2 [25]. Capacity is a function of the compressive strength of the concrete and yield strength of the reinforcing steel [40]. Therefore, it was necessary to calculate these strengths as temperature increased. The compressive strength of concrete decreases at elevated temperatures as a function of Equation 3 [2].

Equation 3: Compressive strength as temperature increases [37]

$$f'_{cT} = \begin{cases} f'_c & T \leq 100℃ \\ f'_c(1.067 - 0.00067T) & 100℃ \leq T \leq 400℃ \\ f'_c(1.44 - 0.0016T) & T \geq 400℃ \end{cases}$$

The decrease of yield strength over temperature has been tested and documented through Topcu and Karakurt's "Properties of Reinforced Concrete Steel Rebars Exposed to High Temperatures" research [41]. S420 steel was used in the column design for this project, shown with hollow diamonds in Figure 20.

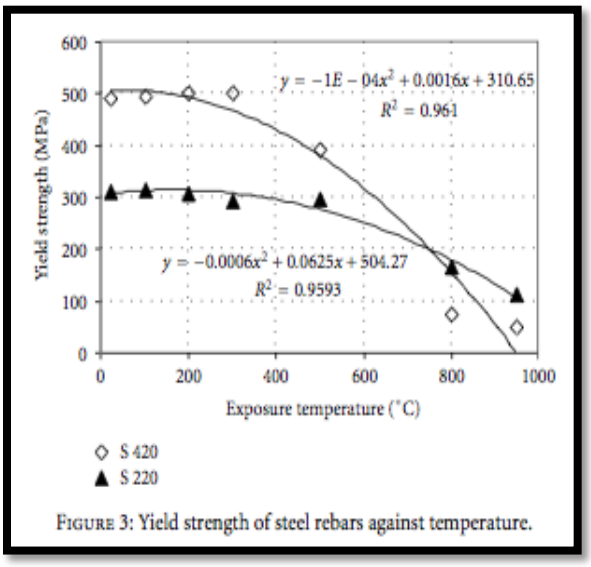

Figure 20: Loss of yield strength over temperature [41]

The temperature of the reinforcing steel is dependent on the heat transfer through the concrete medium. As a simplification, this study models the yield strength as a function of the gas temperature, ignoring the insulating capabilities of concrete. In reality, for steel protected by concrete cover, the gas temperatures are significantly higher than the temperatures at the actual

location of the steel for each spalling scenario. Consequently, the loss of yield strength is overestimated in this work and the steel capacity losses are conservative. The elevated temperature capacities were then displayed as percentages of the original capacity, calculated using

Plots of "Temperature versus Capacity Losses" were created with separate curves for capacity losses due to the concrete, steel, and combined capacity losses on the same axes. The separate curves promote comparisons between the capacity losses of the concrete and steel in relation to the total capacity loss. The capacity losses can be calculated using Equation 4 and Equation 5.

Equation 4: Capacity Loss

$$Capacity\ Loss = Initial\ Capacity - New\ Capacity$$

Equation 5: Capacity Loss as a percent

$$\%\ Capacity\ Loss = \frac{(Initial\ Capcity - New\ Capacity)}{Initial\ Capacity}$$

The initial capacity refers to the capacity at ambient temperature and the new capacity refers to the capacity at elevated temperatures.

4 Results

There is a large amount of research that claims spalling is a bigger concern in HSC [3] than NSC at elevated temperatures. This MQP models both HSC and NSC to assess specific temperatures and pore pressures at which spalls may occur. Comparisons between the results for NSC and HSC not only test if the model works conceptually, but they also give insight to the reasons that HSC spalls to a greater extent than NSC. Typical results which would be indicative of a successful pore pressure model would show elevated pore pressure values for HSC columns over time and increased temperature.

The model described in the Methodology was applied to actual reinforced concrete column designs. A normal strength concrete and high strength concrete column were designed, according to *ACI 318* (described in depth in Appendix B). A series of about 100 column designs were created using varying dimensions, strengths, reinforcement sizes, and number of reinforcements. The dimensions for the column design were based on mid-sized column dimensions, or about 20 inches by 20 inches. These dimensions were chosen because they allowed for an assortment of reinforcement types and sizes to be used within the range of permissible values for reinforcement ratio (refer to Equation 8). Columns were chosen for this model by personal preference for the allowable capacity of the member. In this case, columns with relatively high allowable capacities were selected to see if elevated temperatures would reduce their capacity significantly. Presented in the results are only two columns which were selected as illustrative examples. Table 1 displays the properties for each of these columns. The process used to create and analyze the results is shown in the flow chart in Figure 21.

Table 1: Design Parameters for NSC and HSC at ambient temperatures [25]

	NSC	HSC
Size	20in. by 20in.	20in. by 20in.
Compressive Strength	35MPa (5,000psi)	110MPa (16,000psi)
Tensile Strength	2MPa (283psi)	3.5MPa (506psi)
Yield Strength	414MPa (60,000psi)	414 MPa (60,000psi)
W/C	0.48	0.30
Cement Type	Portland Cement Type I	Portland Cement Type I
Aggregate Size	19mm (0.75in.)	19mm (0.75in.)
Steel Reinforcements	Deformed Steel	Deformed Steel
Admixtures	None	None
Cover	38mm (1.5in.)	38mm (1.5in.)
Reinforcements	4 #9 bars	4 #9 bars

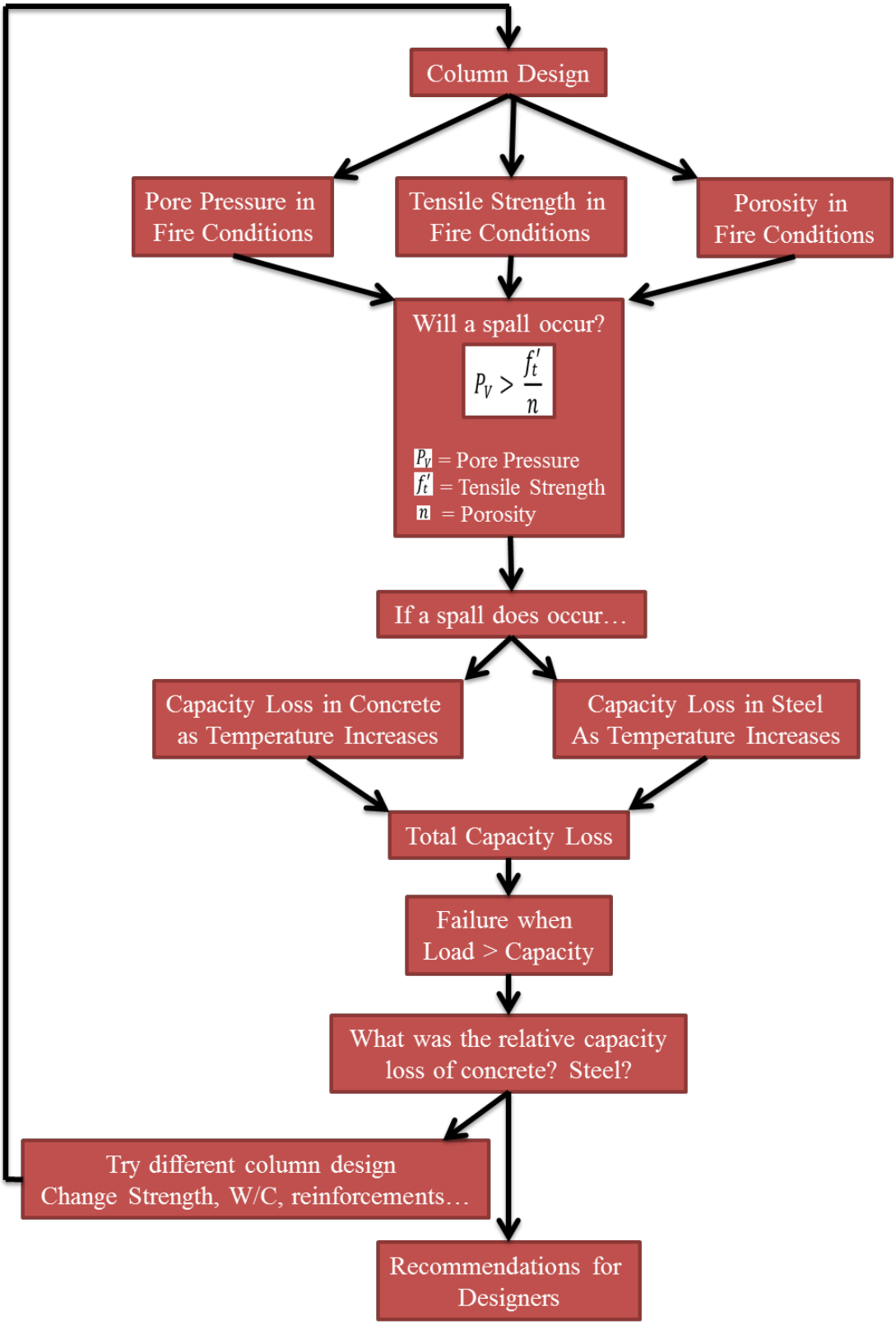

Figure 21: Results Flow Chart

4.1 Predicting a Spall

Recall from the methods section that Kodur's "Hydrothermal model for predicting fire-induced spalling in concrete structural systems" [3] provided graphs pertaining to time, temperature, and pore pressure. Figure 16 displays time-temperature curves at various depths of a concrete slab from Kodur's analysis. Interpolation was performed on these curves to estimate time-temperature curves at three desired depths: 20mm, 30mm, and 40mm from the exposed surface (shown in Figure 22). A regression analysis was performed for data at these depths because Kodur provides data on the pore pressures at these depths [3].

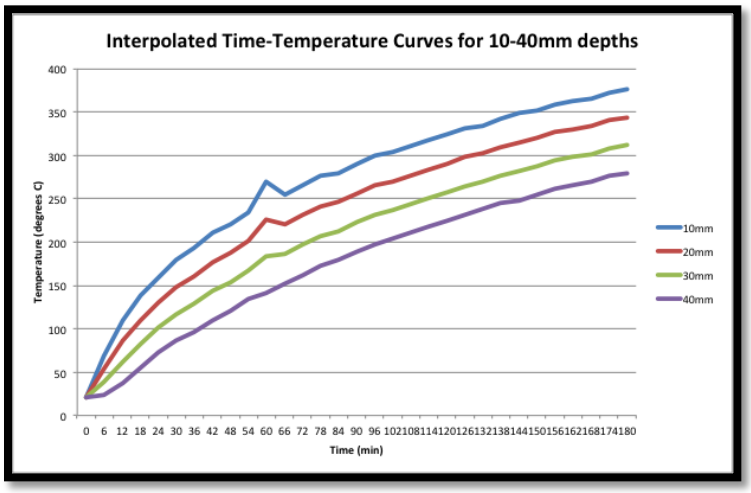

Figure 22: Interpolated time-temperature curves at depths of 10mm, 20mm, 30mm and 40mm from the exposed surface

These time-temperature curves and Kodur's "Time versus Pore Pressure" curves were based on the *ASTM E119* [38] standard fire curve. These curves were combined to create "Temperature versus Pore Pressure" relationships. There was sufficient data to form these relationships for concrete at depths of 20mm, 30mm, and 40mm from the exposed surface (Figure 23 shows this relationship at a depth of 20mm).

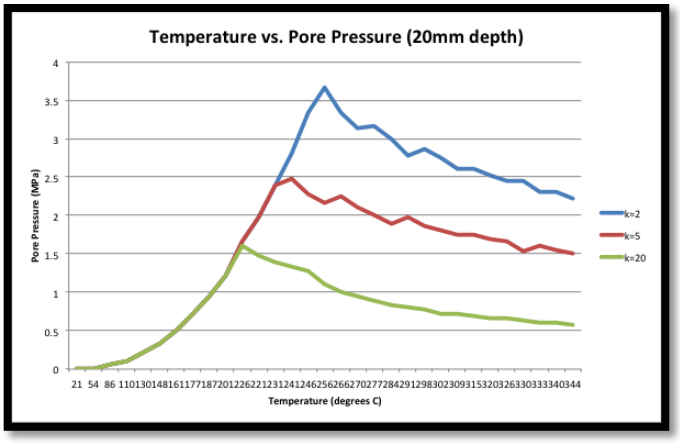

Figure 23: Temperature versus Pore Pressure at a depth of 20mm from the exposed surface

As explained in the Methodology, "Temperature versus Pore Pressure" can be plotted on the same axes as "Temperature versus $\frac{f_t'}{n}$". The point of intersection between these curves represents the temperature and pore pressure a spall will occur. Figure 24 shows these curves for a NSC with a permeability of $2 \times 10^{-18} m^2$ at depths of 20mm, 30mm, and 40mm from the exposed surface.

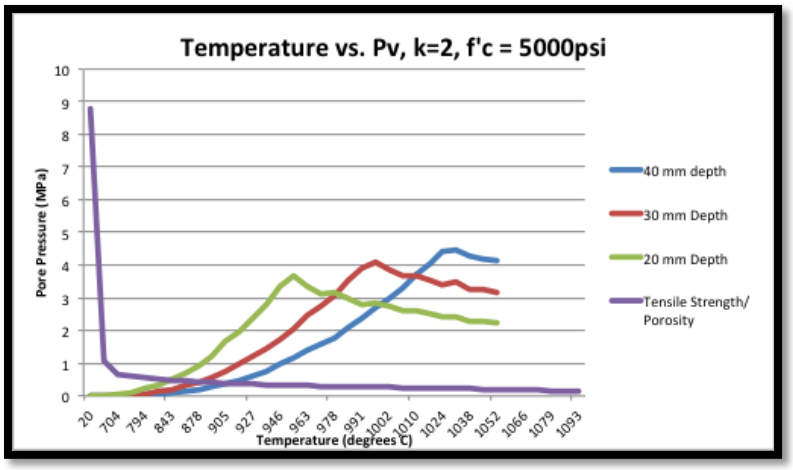

Figure 24: Pore pressure and loss of tensile strength as temperature increases

Figure 24 shows the pore pressure and tensile strength as a function of the temperature of the gas (or furnace). Figure 25 provides context for the temperature values at depth (20mm spalling scenario is presented here), showing that they lag the surface temperature due to the mechanics of heat transfer and insulation properties of the concrete.

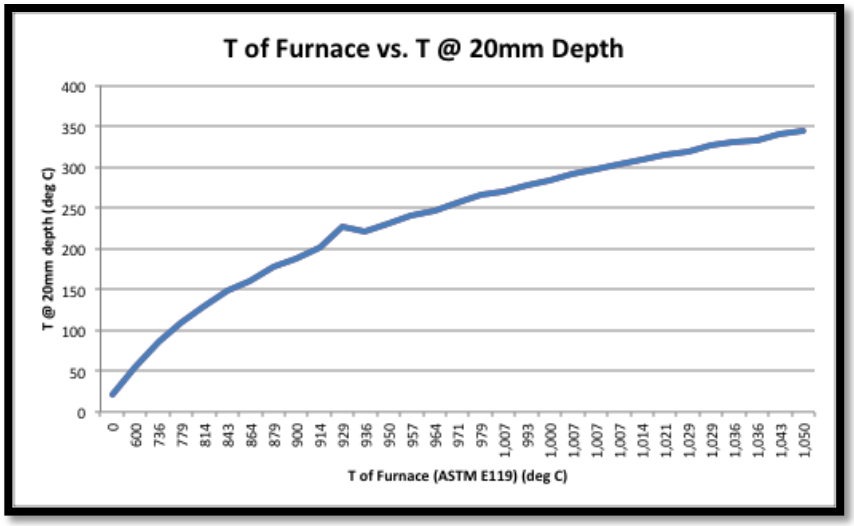

Figure 25: Furnace temperature *(ASTM E119* standard fire curve) versus temperature at a depth of 20mm from the exposed surface

Figure 26 is a maximized view of the points of intersection for the pore pressure curves and the $\frac{f_t'}{n}$ curve for the NSC curves in Figure 24. The points of intersection between each pore pressure curve (blue, red, and green) and the $\frac{f_t'}{n}$ curve (purple) represent the temperature and pore pressure at which spalling may occur at that respective depth.

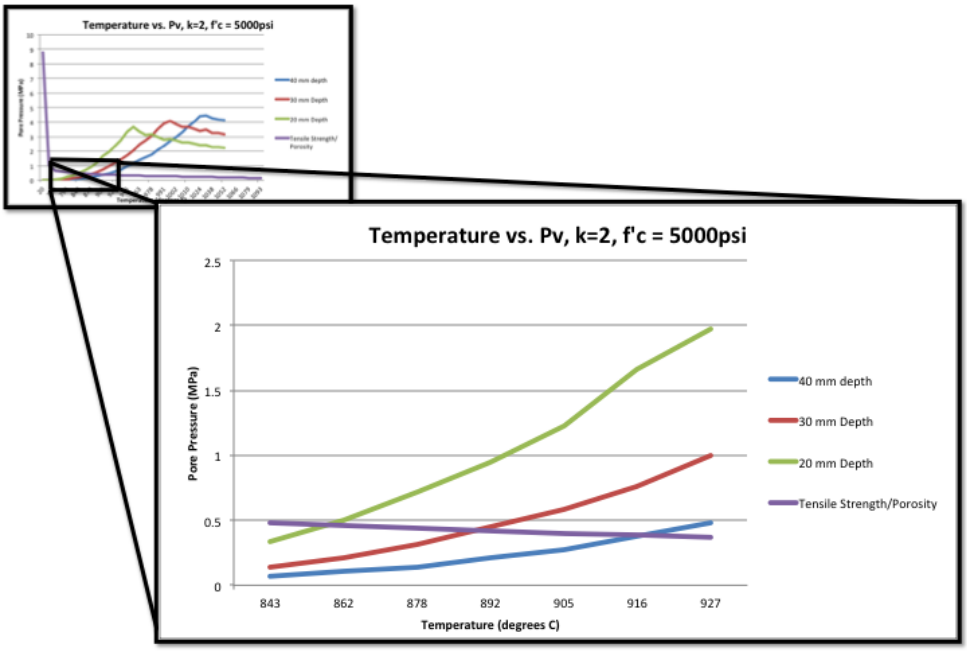

Figure 26: Points of intersection for pore pressure and loss of tensile strength curves at various depths of NSC

Figure 27 shows temperatures and pore pressures that a spall will occur at for NSC and HSC with a permeability of $2 \times 10^{-18} m^2$ at a depth of 20mm.

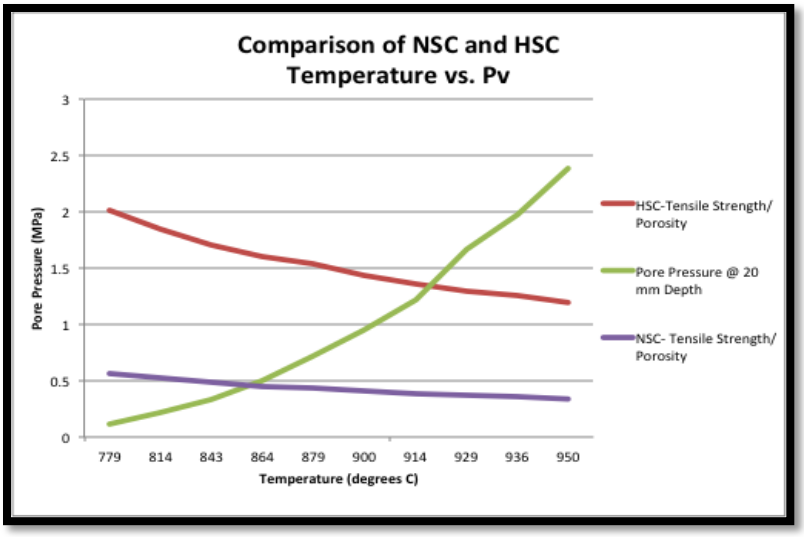

Figure 27: Points of intersection between pore pressure and tensile strength/porosity for NSC and HSC at a depth of 20mm from the exposed surface

Data for the comparison between NSC and HSC at depths of 20mm, 30mm, and 40mm is tabulated in Table 2.

Table 2: Approximate temperatures that a spall will occur for NSC and HSC at various depths from the exposed surface

Depth from Exposed Surface (mm)	Pore Pressure when $P_V > \frac{f_t'}{n}$		Temperature when $P_V > \frac{f_t'}{n}$	
	NSC (MPa)	HSC (MPa)	NSC (degrees C)	HSC (degrees C)
20mm	0.45	1.3	860	920
30mm	0.4	1.2	890	950
40mm	0.35	1.1	920	970

This table shows that HSC will spall at a higher temperature and pore pressure than NSC. This would lead some to believe that HSC would have a lower propensity to spall. However, HSC is more prone to explosive spalling- "a sudden and violent breaking away of a surface layer of concrete" [42].

Kalifa [43] describes the spalling process of HSC

> "…as a thermo-hydral process which is associated with the transfer of mass in the concrete's porous network (air, vapor, liquid water), which results in the buildup of high pore pressures and pore pressure gradients [43]."

Essentially, this process is attributed to HSC's low permeability and its inability to successfully mitigate the buildup of internal pressure [44]. Table 2 shows that HSC does not spall until it reaches a higher temperature and pore pressure than NSC. Although a spall in HSC doesn't occur until a higher temperature than NSC, the magnitude of the spall will be greater because the pore pressure is higher. This observation is in agreement with the large amount of research on spalling, which claims spalling is worse in HSC [44].

This study has demonstrated a framework for predicting spall and has provided temperatures for a spall to occur. For example, NSC should spall at a depth of 20mm from the exposed surface when the furnace temperature reaches approximately 860 degrees Celsius (or 35 minutes into an *ASTM E119* standard fire test). Although these types of predictions are insightful, they do not tell the whole story. Assuming spalls do occur, how much will that affect the structural integrity of a member?

4.2 Capacity Losses

Fire-induced spalling causes losses of cross section, which diminishes the column's load capacity. Quantifying these losses is critical to understanding the impact of spall on the structural integrity of reinforced concrete members.

The capacity model was applied to the NSC and HSC column design; the fire exposure was assumed to be uniform on all sides of the column. Equation 6 is the ultimate capacity equation for a reinforced concrete column; it was used to calculate capacity losses of the NSC and HSC columns for several spalling scenarios.

Equation 6: Ultimate Capacity Equation for a Reinforced Concrete Column [40]

$$P_n = [.85f_c'(A_{conc}) + f_y'(A_{st})](\phi)(\alpha)$$

Where:

- P_n = Ultimate Capacity
- f_c' = Compressive Strength
- A_{conc} = Net Area of Cross Section (Cross Sectional Area – Area of Steel)
- f_y' = Yield Strength of Steel
- A_{st} = Area of Steel
- ϕ = .65 For axial compression members with or without flexure
    - Strength Reduction Factor for Concrete
- α = .80 Accounts for unintended eccentricity or bending moment
    - Strength Reduction Factor for Concrete

The losses of tensile, yield, and compressive strength with elevated temperatures were modeled, as discussed in Chapter 3 Methodology. Relationships between temperature and capacity loss individually caused by the concrete and reinforcing steel, as well as the combined capacity losses are presented in this section. These comparisons demonstrate which element is a greater contributor to capacity losses during a fire exposure. Although these comparisons are valuable, they should be considered with caution. The unique and changing loading conditions of a member in fire conditions affects the maximum allowable capacities of the concrete and steel. If a column is loaded axially and loses the capacity of its reinforcing steel at a high rate, the overall structural integrity of the column may be satisfactory because the concrete may have sufficient capacity to support the compressive load. However, beams that lose tensile capacity at a high rate will experience serious structural issues because the reinforcing steel is central to resisting the bending moments caused from point and distributed loads.

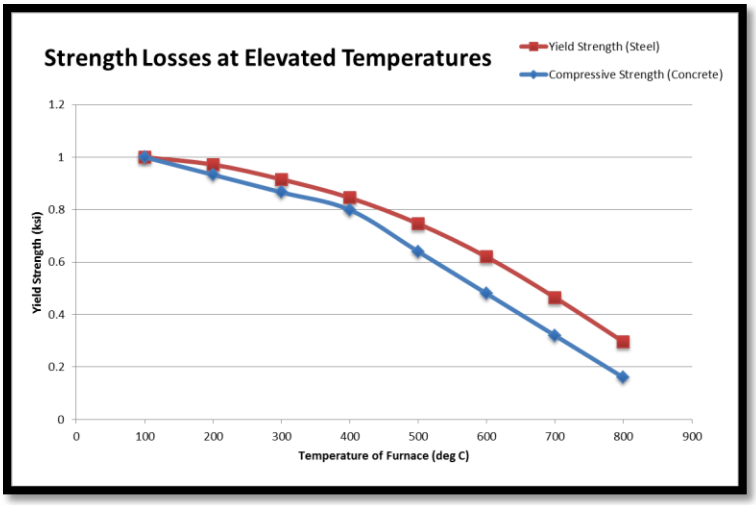

Figure 28: Strength Losses at Elevated Temperatures

Figure 28 displays how both concrete and steel strengths degrade at elevated temperatures. To be clear, the left axis is a ratio of new capacity divided by the initial capacity at elevated temperatures; this ratio normalizes the temperature-dependent values for normal conditions so that both materials could be placed on the same axes. This figure shows that concrete and steel maintain a similar rate of capacity loss until a temperature of about 400ºC is reached. As temperatures exceed 400ºC, the compressive strength of concrete declines at a greater rate. This result mirrors that of the capacity losses for NSC and HSC as shown in Figure 29 and Figure 30.

Figure 29 shows the capacity curves for concrete, steel, and total capacity losses plotted on the same axes to illustrate the relative contribution of compressive and yield strength losses to the total capacity loss. This figure represents a column without spalling (no cross section losses) and each capacity curve begins at 100% capacity. The concrete loses capacity at a higher rate than the reinforcing steel. We must remember the limitations of this model when these capacity loss graphs. The model ignores the insulating capabilities of concrete and uses the gas temperatures to calculate the loss of yield strength in the reinforcing steel. The steel capacity loss curve in Figure 29 actually models exposed steel (40mm spalling, shown in Figure 30) so its decay rate is overestimated. The capacity losses are conservative for each spalling scenario except for the 40mm spall which represents exposed reinforcing steel. Even with this conservation, the concrete capacity losses are greater than the steel capacity losses.

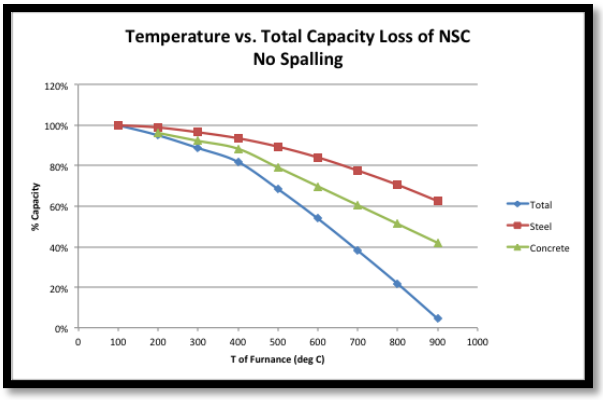

Figure 29: Temperature versus Percent Capacity Loss of NSC (No Spalling)

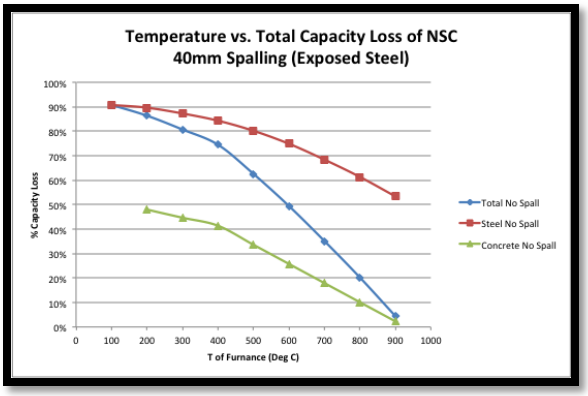

Figure 30: Temperature versus Total Capacity Loss of NSC (40mm Spalling: Exposed Steel)

The reduced concrete cross-section causes the initial concrete capacity to be less than 50% of its original capacity before a significant temperature rise. The model accurately calculates the steel capacity loss for this scenario because of the model's use of gas temperatures for yield strength values and the steel is exposed after the concrete spalls in this scenario. Figure 30 shows the impacts that significant spalling can have on a reinforced concrete column. A point of failure is not identified because loading conditions are not specified. This enables designers to use this model to analyze their loading conditions by determining the percent capacity loss that would pose serious structural issues. Ultimately, this knowledge could help designers determine the factor of safety necessary to appropriately protect against spalling.

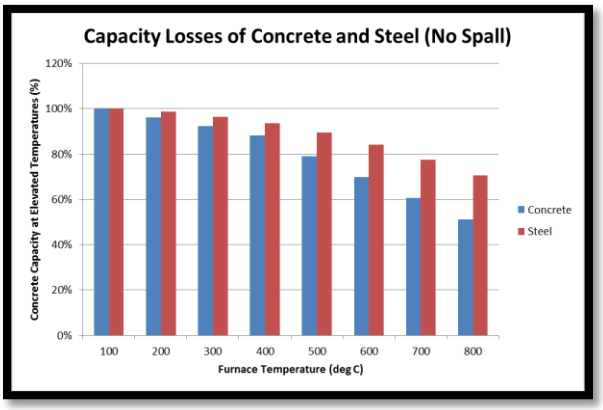

Figure 31: Capacity Losses of Concrete and Steel (No Spall)

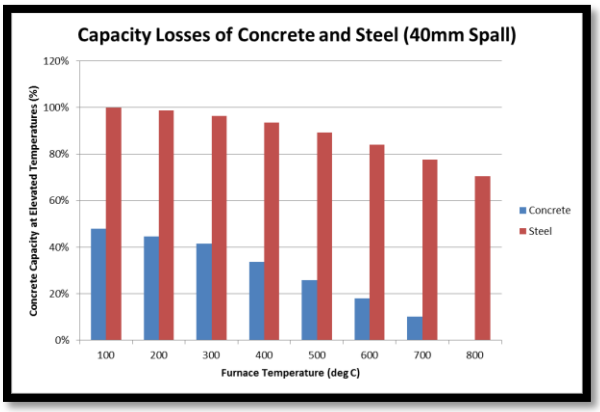

Figure 32: Capacity Losses of Concrete and Steel (40mm Spall)

Figure 31 and Figure 32 compare the capacity losses from the concrete and steel of a NSC column with no spalling to a NSC column with 40mm spalling (exposed steel). These figures show that the column with a spall loses concrete capacity at a much higher rate than the column with no spalling due to the loss of concrete cross section associated with the spall. These figures assist in validating the model described herein by showing that spalling has a significant effect on member capacity. Information such as this is beneficial to helping a designer choose the appropriate column with known loading conditions.

5 Conclusions

Analysis indicates that a HSC column begins to spall at a higher temperature than the NSC column, as shown in Figure 27. Reiterating the pore pressure phenomena, Table 2 displays the times and temperatures a spall may occur for NSC and HSC, according to this model. The pore pressure values for HSC are nearly three times as high as those for NSC at various depths. The temperatures are approximately 60 ºC higher for the HSC than for NSC. From this data it can be concluded that a NSC member may spall sooner, but it is at a much smaller magnitude than that of a HSC member. With such a high pore pressure, longer lag time to spall, and higher temperature, the HSC spalls more explosively. This spall will affect the capacity of the member more than a spall of a NSC member. This is consistent with the information known about HSC columns.

Figure 29 and Figure 30 show the total capacity losses for a column without spalling and a column with 40 mm of spalling. The capacity of the concrete column without any spalling is 100% at 100 ºC and gradually decreases until it reaches 40% capacity at 900ºC. In contrast, the capacity of the concrete with 40 mm of spalling, which represents a column with exposed steel, has 50% capacity at 100 ºC and decreases to 0% capacity at 900ºC. This comparison demonstrates the importance of the concrete cover protection for the overall capacity of a member. This data does not suggest that a spall has already occurred at 100ºC, but rather shows a relationship to the cross-sectional loss of the concrete, capacity, and temperature. For these studies the concrete was more of a governing factor than the steel.

According to Figure 31 and Figure 32, a column with a spall loses concrete capacity at a much higher rate than the column with no spalling due to the loss of concrete cross section associated with the spall. These figures assist in validating the model described herein by showing that spalling has a significant effect on member capacity.

6 Future Work

The model in this study calculated the yield strength of the reinforcing steel as a function of gas temperature. The model did not account for the insulating capabilities of concrete; it was conservative by assuming uniform temperature across the section, and the temperature was assumed to be equal to that of the furnace. In reality, the temperatures of the steel for columns without spalling, and with 20mm and 30mm spalls are lower than the values used in this model. A heat transfer analysis to determine the temperatures of the steel at various depths from the exposed surface would improve the model. Accurate values for the steel temperature would enable more accurate capacity loss relationships to be made. Better comparisons could be made between the capacity losses from concrete and steel as well.

Expressing the validity of the model through other data sets would be beneficial. Data sets similar to Kodur's data for pore pressure could be run through the model to check validity of the entire system against different information. Also, being able to validate Kodur's relationships for pore pressure based on slabs against this models relationships to columns could help to normalize spalling in all types of concrete members. Assembling a database to incorporate similar models would also help to keep all known information about spalling research together.

The model could be run with a larger variety of column types and designs to identify relationships between column types, reinforcement placements, materials, etc. For example, a column using air-entraining admixtures could be created. To incorporate this in this model, however, there would need to be sufficient data on how air-entraining admixtures affect concrete properties at elevated temperatures. For such data to be available there would need to be further laboratory data accessible to understand the effects certain concrete admixtures may have on the concrete's properties, pore pressure, and porosity at elevated temperatures.

The specific fire environment concrete is exposed to, has a direct effect on the propensity of the concrete to spall. Fires with high HRR, such as hydrocarbon fires (*ASTM E1529)*, cause temperature gradients to form at the surface because the heat does not have sufficient time to diffuse to the inner layers of concrete [34] and the temperature differentials can cause spalling. It would be valuable to apply the model to other fire environments to predict spalling and its effects in varying conditions.

7 Bibliography

[1] International Building Code, 2011 International Building Code, Country Club Hills: IBC, 2011.

[2] Eurocode, Eurocode 2: Design of Concrete Structures - Part 1-2: General Rules - Structural Fire Design, Brussels: European Concrete Platform, 2004.

[3] V. Kodur and M. Dwaikat, "Hydrothermal Model for Predicting Fire-Induced Spalling in Concrete Structural Systems," *Fire Safety Journal,* vol. XLIV, no. 3, pp. 425-434, 2009.

[4] Portland Cement Association, "Cement & Concrete Basics," Portland Cement Association, 2012. [Online]. Available: http://www.cement.org/basics/howmade.asp. [Accessed 10 December 2011].

[5] American Society for Testing and Materials, Standard Specification for Portland Cement, West Conshohocken: ASTM International, 2009.

[6] S. Chandra and L. Berntsson, Lightweight Aggregate Concrete Science, Technology, and Applications, Norwich: Noyes Publications, 2002.

[7] M. D'Ambrosia and N. Mohler, "Introduction to Civil Engineering Materials," 12 August 2010. [Online]. Available: http://sab2112.blogspot.com/. [Accessed 15 December 2011].

[8] Federation Internationale Du Beton, Fire Design of Concrete Structures - Materials, Structures and Modeling, Lausanne: International Federation for Structural Concrete, 2007.

[9] V. K. R. Kodur and M. A. Sultan, "Effect of Temperature on Thermal Properties of High-Strength Concrete," *Journal of Materials in Civil Engineering,* vol. XV, no. 2, pp. 101-107, 2003.

[10] V. R. Kodur and M. A. Sultan, Structural Behaviour of High Strength Concrete Columns Exposed to Fire, Sherbrooke: International Symposium on High Performance and Reactive Powder Concrete, 1998.

[11] NORCHEM, "How Does Silica Fume Work in Concrete?," NORCHEM, 2011. [Online]. Available: http://www.norchem.com/silica-fume-concrete.html. [Accessed 4 December 2011].

[12] American Concrete Institute, "Chemical Admixtures for Concrete," American Concrete Institute, Farmington Hills, 2003.

[13] V. Kodur and R. McGrath, "Effect of silica fume and lateral confinement on fire endurance of high strength concrete columns," *Canadian Journal of Civil Engineering*, vol. 33, pp. 93-102, 2006.

[14] Kentucky Ash, "Evaluating Fly Ash for Concrete," Kentucky Ash, 2010. [Online]. Available: http://www.caer.uky.edu/kyasheducation/testing-concrete.shtml. [Accessed 17 November 2011].

[15] Clean Energy Exhibition, "The Next Generation Solar Home," [Online]. Available: http://solar.world.org/solar/concrete. [Accessed 8 December 2011].

[16] TK Products, "Curing Concrete," TK Products, Minnetonka.

[17] AboutCivil.com, "Properties of Concrete," SJ Soft Technologies, 2010. [Online]. Available: http://www.aboutcivil.com/Properties-of-concrete-factors-affecting-them.html. [Accessed 9 December 2011].

[18] American Concrete Institute, "Durability - Carbonation," ACI, 26 June 2006. [Online]. Available: http://www.concrete.org/FAQ/afmviewfaq.asp?faqid=50. [Accessed 28 February 2012].

[19] Cement Concrete & Aggregates Australia, "Concrete Basics A Guide to Concrete Practice," CCAA, Sydney, 2004.

[20] MultiQuip, "Concrete Vibration Handbook," MultiQuip Inc., Carson.

[21] Big Boss F.Z.E., "Steel Bars," BBGT, 2011. [Online]. Available: http://bigbossgulf.com/steel-bars. [Accessed 10 December 2011].

[22] American Concrete Institute, "Reinforcement for Concrete - Materials and Applications," American Concrete Institute, Farmington Hills, 2006.

[23] NEITC, "Reinforcing Steel Placement Handbook," NEITC, 1999.

[24] Concrete Basics, "Placement of Reinforcing Steel," Concrete - Techgroup, 2008. [Online]. Available: http://www.concretebasics.org/articlesinfo/placementreinfsteel.php. [Accessed 28 February 2012].

[25] American Concrete Institute Commitee 318, Building Code Requirements for Structural Concrete and Commentary, Farmington Hills: American Concrete Institute, 2010.

[26] A. H. Nilson, D. Darwin and C. W. Dolan, Design of Concrete Structures, New York:

McGraw-Hill, 2004.

[27] T. Z. Harmathy, M. A. Sultan and J. W. MacLaurin, "Comparison of Severity of Exposure in ASTM E119 and ISO 834 Fire Resistance Tests," *Journal of Testing and Evaluation,* vol. VI, no. 6, pp. 371-375, 1987.

[28] M. Li, Z. Wu, H. Kao, C. Qian and W. Sun, "Calculation and Analysis pf Pore Vapor Pressure of Concrete Exposed to Fire," *International Journal of the Physical Sciences,* vol. V, no. 8, pp. 1315-1323, 2010.

[29] J. L. Rhoads, "Basic Explanation of Creep Processes," University of California, Berkeley, 17 June 2008. [Online]. Available: http://web.archive.org/web/20080617053739/http://www.nuc.berkeley.edu/thyd/ne161/jlrhoads/creep.html. [Accessed 2 December 2011].

[30] V. K. Kodur and T. Z. Harmathy, "Properties of Building Materials," in *The SFPE Handbook of Fire Protection Engineering*, Quincy, National Fire Protection Association, 2008.

[31] O. M. Jensen and P. F. Hansen, "Water-Entrained Cement-Based Materials: Principles and Theoretical Background," *Cement and Concrete Research,* vol. XXXI, no. 4, pp. 647-654, 2001.

[32] G. A. Somorjai and Y. Li, Introduction to Surface Chemistry and Catalysis Second Edition, Hoboken: John Wiley & Sons, Inc., 2010.

[33] M. Shamalta, A. Breunese, W. Peelen and J. Fellinger, "Numerical modelling and experimental assessment of concrete spalling in fire," *HERON,* vol. 50, no. 4, pp. 303-319, 2005.

[34] J.-C. Mindeguia, P. Pimienta, A. Noumowe and M. Kanema, "Temperature, Pore Pressure and Mass Variation of Concrete Subjected to High Temperature - Experimental and Numerical Discussion on Spalling Risk," *Cement and Concrete Research,* vol. XL, no. 3, pp. 477-487, 2010.

[35] M. G. Hernandez, M. A. Izquierdo, A. Ibanez, J. J. Anaya and L. G. Ullate, Porosity Estimation of Concrete by Ultrasonic NDE, Elsevier Science, 2000.

[36] American Society of Civil Engineers (ASCE), Structural Fire Protection, Manual No. 78, New York: ASCE, 1992.

[37] M. Bastami, F. Aslani and M. Esmaeilnia Omran, "High-Temperature Mechanical

Properties of Concrete," *International Journal of Civil Engineering,* vol. VIII, no. 4, pp. 337-351, 2010.

[38] American Society of Testing and Materials, Standard Test Methods for Fire Tests of Building Construction and Materials, West Conshohocken: ASTM International, 2012.

[39] T. L. (Ed.), Structural Fire Protection, New York: American Society of Civil Engineers, 1992, p. 78.

[40] J. Ochshorn, Structural Elements for Architects and Builders, Burlington: Butterworth-Heinemann, 2009.

[41] I. B. Topcu and C. Karakurt, Properties of Reinforced Concrete Steel Rebars Exposed to High Temperatures, Eskisehir: Hindawi Publishing Corporation, 2008.

[42] U. Diederichs, U. M. Jumppanen and U. Schneider, "High Temperature Properties and Spalling Behavior of High Strength Concrete," *Proceedings, Fourth Weimar Workshop on High Performance Concrete: Material Properties and Design,* pp. 219-239, 1995.

[43] P. Kalifa, F.-D. Menneteau and D. Quenard, "Spalling and Pore Pressure in HPC at High Temperatures," *Cement and Concrete Research,* vol. XXX, pp. 1915-1927, 2000.

[44] L. Phan, Spalling and Mechanical Properties of High Strength Concrete at High Temperature, Gaithersburg: National Institute of Standards and Technology, 2007.

[45] R. J. Davis, Fire Protection Handbook, Quincy: National Fire, 2008.

[46] ArupFire, Fire Resistance of Concrete Enclosures, London: Arup Group, 2005.

[47] B. K. Venkanna, Fundamentails of Heat and Mass Transfer, New Delhi: PHI Learning Private Limited, 2010.

[48] "Table 7-1: U.S. STandard Reinforcing Bars," Integrated Publishing, 2011. [Online]. Available: constructionmanuals.tpub.com/14251/css/14251_189.htm. [Accessed 23 01 2012].

[49] American Concrete Institute, Building Code Requirements for Structural Concrete and Commentary, Farmington Hills: American Concrete Institute, 2008.

[50] L. T. Phan, "Pore Pressure and Explossive Spalling in Concrete," *Materials and Structures,* vol. XLI, pp. 1623-1632, 2008.

[51] T. Z. Harmathy, "Fire Safety Design and Concrete," Longman Scientific and Technical, United Kingdom, 1993.

[52] G. Giacco and R. Zerbino, "Failure Mechanism of Concrete: Combined Effects of Coarse Aggregates and Strength Level," *Advanced Cement Based Materials*, vol. VII, no. 2, pp. 41-48, 1998.

[53] V. K. Kodur and T. Z. Harmathy, "Properties of Building Materials," in *SFPE Handbook of Fire Protection Engineering*, Quincy, National Fire Protection Association, 2002.

8 Appendix

Appendix A

A.1 Thermal Properties

The following section is an encyclopedic collection of the various thermal properties of concrete that affect the propensity to spall, including thermal conductivity, specific heat, thermal diffusivity, thermal expansion, and density.

A.1.1 Thermal Conductivity

The thermal conductivity (k) is the ability of a material to conduct heat. Concrete has a relatively low thermal conductivity which decreases with elevated temperatures. At ambient temperatures, the thermal conductivity of normal strength ordinary concrete is 0.8~2.6W/mK; this decreases to a range of 0.5~1.3W/mK at a temperature of 1000ºC. This decrease in thermal conductivity actually decreases the concrete's propensity to spall because the heat does not transfer through the concrete as quickly. The low thermal conductivity of concrete also causes the distribution of temperatures to be poor, see Figure 33. It should also be noted that light weight concrete has a lower coefficient of thermal conductivity than normal weight concrete which makes it less susceptible to spalling at elevated temperatures [45].

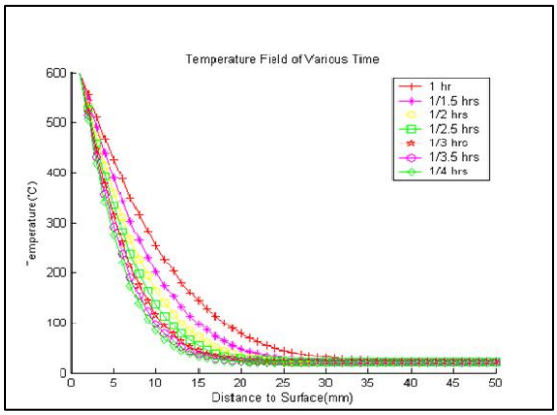

Figure 33: Temperature field different heating times [28]

A.1.2 Specific Heat

Specific heat (c_p) is the amount of heat necessary to increase the temperature of a material by 1ºC. The specific heat of concrete increases with elevated temperatures; the range for specific heat at ambient temperature is 750~920J/kgK and 930~1230 at 1000ºC. The specific heat is not greatly impacted by the type of aggregate, unlike other thermal properties.

A.1.3 Density

The density of concrete is imperative when investigating spalling. Density is related to permeability which, in turn, is related to pore pressure. The increase of pore pressure is a fundamental mechanism of spalling. The density of concrete at ambient temperature is 2000~2600kg/m^3, while the density of concrete at 900ºC is 1500~2300kg/m^3 [46].

A.1.4 Thermal Diffusivity

Thermal diffusivity describes the ability of heat to travel through a material during a dynamic process. Thermal diffusivity can be found by dividing the thermal conductivity (k) by the volumetric heat capacity (product of the specific heat (c_p) and density (ρ) of concrete) (see Equation 7). Thermal diffusivity increases with increasing temperatures.

Equation 7: Thermal Diffusivity [47]

$$\propto = \frac{k}{c_p * \rho}$$

A.1.5 Thermal Expansion

Thermal expansion is the tendency of a material to change in volume in response to a change of temperature. Depending on the rate of heating, the degree of thermal expansion can be significant enough to cause spalling. This is especially true if the coefficient of thermal expansion increases for the concrete and reinforcing steel at different rates. Figure 34 shows the thermal expansion for steel and concretes with different aggregates as temperature rises for steel.

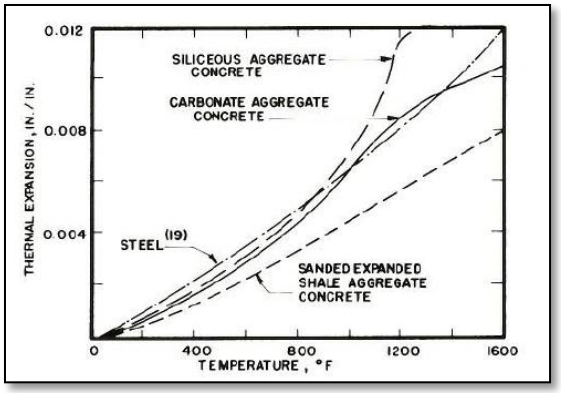

Figure 34: Thermal and Concrete at High Temperatures Expansion of Steel [30]

Appendix B

B.1 Column Design

To investigate this phenomenon properly it was essential to examine the current codes which regulate the design of a concrete member in the United States as to create a reinforced column applicable to the pore pressure model presented. Both Normal Strength and High Strength concrete columns were created to test the model against. Multiple designs were completed and checked with the proper equations to ensure their validity (Sample calculations are provided below). Through the use of active spreadsheets the column design could be changed to influence the capacity loss values for both steel and concrete.

The materials considered when designing this column include cement types, fine and coarse aggregate sizes, water, reinforcing steel, and the addition of air-entraining admixtures. The materials chosen based on the ACI constraints for columns subject to an interior environment are as follows:

B.1.1 Cement Type

Portland Cement Type I: Type I is a general purpose portland cement suitable for all uses where the special properties of other types are not required. It is used where cement or concrete is not subject to specific exposures, such as sulfate attack from soil or water, or to an objectionable temperature rise due to heat generated by hydration. Its uses include pavements and sidewalks, reinforced concrete buildings, bridges, railway structures, tanks, reservoirs, culverts, sewers, water pipes and masonry units [25]

.

B.1.2 Aggregate Type & Size

For the purposes of this investigation an aggregate type was not chosen because of the lack of ability of experimentation. Venkatesh Kodur is at the forefront of spalling research and has noted that the two main types of concrete aggregate (carbonate and siliceous) differ in their thermal expansion and fire resistance. Carbonate being the stronger of the two materials has been known to resist higher temperatures than other aggregate types. For this study a normal weight aggregate of size 19 mm (.75 in.) was chosen. This value can be also be found in *ACI 318* and is constant for both NSC and HSC.

B.1.3 Steel Reinforcement Size & Quantity

Deformed steel reinforcements will be used throughout this model because they are the most widely used type of steel bar in reinforced concrete construction [25]. Other reinforcements, like fibers are beneficial to the fire resistance of HSC. To visualize the effects of fire on both NSC and HSC the steel reinforcements were also kept constant throughout. Considering a concrete column cross section of 500 mm by 500 mm (20 in. by 20 in.), the number and size of the steel bars is evaluated through a series of capacity equations and reinforcement ratio checks. Equation 8 shows the reinforcement ratio for steel bars. The ratio must be within 1% and 8%. Calculations showing these methods are provided at the end of this section.

$$P_g = \frac{A_{st}}{A_g}$$

Equation 8: Reinforcement Ratio [40]

Where:

- P_g = Reinforcement Ratio
- A_{st} = Area of Steel
- A_g = Gross Cross Sectional Area

B.1.4 Steel Yield Strength

S420, or more commonly known as S60 steel bars have a yield strength of 414 MPa (60,000 psi). This is a common value for reinforcing bars and will be used to represent the yield strength in both the NSC and HSC of this model; f_y' represents yield strength in the capacity equations.

B.1.5 Air-Entraining Admixtures

Air-entrainment is used in concrete design for columns that undergo a constant cycle of freezing and thawing. These admixtures are normally used for exposure classifications F1-F3. In this case there is no air-entrainment needed because this column design is exposure classification F0. Because this column will only be exposed to an interior environment there is no need to protect against freezing and thawing. The difference between exposure classifications can be seen in Figure 35.

TABLE 4.3.1 — REQUIREMENTS FOR CONCRETE BY EXPOSURE CLASS

Exposure Class	Max. w/cm*	Min. f'_c, psi	Additional minimum requirements			
			Air content			Limits on cementitious materials
F0	N/A	2500	N/A			N/A
F1	0.45	4500	Table 4.4.1			N/A
F2	0.45	4500	Table 4.4.1			N/A
F3	0.45	4500	Table 4.4.1			Table 4.4.2
			Cementitious materials†—types			Calcium chloride admixture
			ASTM C150	ASTM C595	ASTM C1157	
S0	N/A	2500	No Type restriction	No Type restriction	No Type restriction	No restriction
S1	0.50	4000	II‡	IP(MS), IS (<70) (MS)	MS	No restriction
S2	0.45	4500	V§	IP (HS) IS (<70) (HS)	HS	Not permitted
S3	0.45	4500	V + pozzolan or slag‖	IP (HS) + pozzolan or slag‖ or IS (<70) (HS) + pozzolan or slag‖	HS + pozzolan or slag‖	Not permitted
P0	N/A	2500	None			
P1	0.50	4000	None			

Figure 35: Exposure Class Requirements for Concrete [25]

B.1.6 Water/Cement Ratio

For a 35 MPa (5,000 psi) NSC column a W/C ratio of .48 will be used in this design. For the HSC with $f'c$ of 110 MPa (16,000 psi) a W/C of .30 was chosen. These values are consistent with *ACI 318* and the exposure classifications these columns fall under. Because the model developed depends on pore pressure, porosity, and tensile strength, it can be seen that water is an important factor in determining a concrete column's propensity to spall.

B.1.7 Concrete Cover

For concrete not exposed to weather or in contact with the ground, the minimum protection for the reinforcement for beams and columns is 1 ½ inches or approximately 38 mm. To investigate the effects of spalling on a column the cover thickness was reduced 10 mm, 20 mm, 30 mm, and 40 mm. The reduced values were also input into the capacity equations to show the various losses. An example is shown below.

B.1.8 Tensile Strength of Concrete

The tensile strength for a normal weight concrete column is determined by this equation:

Equation 9: Direct Tensile Strength for Normal Weight Concrete [25]

$$f_t' = 3 \; to \; 5\sqrt{f_c'}$$

Where:

- f_t' = Tensile Strength
- f_c' = Compressive Strength

Knowing that the compressive strength used in this model will be 35 MPa (5,000 psi) and 110 MPa (16,000 psi), it is easy to determine the concrete's tensile strength.

These are the major materials and values included in a concrete mix which are necessary when attempting to calculate the maximum capacity of the column. Capacity calculations and capacity loss comparisons are displayed below.

Now that the column design is known and all the necessary variables have been discovered, a capacity analysis is necessary to help in predicting at what time in a fire environment a concrete column will spall. The capacity of a concrete column is the total load the column will be able to endure. In a fire environment a column will experience loss of cross section at differing depths which essentially diminishes the column's capacity. A critical point for the concrete is that at which the spall leaves the reinforcements exposed and therefore the yield strength of the steel also begins to diminish. To calculate capacity this equation was used:

Equation 10: Ultimate Load Capacity Equation [40]

$$P_n = [.85f_c'(A_{conc}) + f_y'(A_{st})](\phi)(\alpha)$$

Where:

- P_n = Ultimate Capacity
- f_c' = Compressive Strength
- A_{conc} = Net Area of Cross Section (Cross Sectional Area – Area of Steel)
- f_y' = Yield Strength of Steel
- A_{st} = Area of Steel
- ϕ = .65 For axial compression members with or without flexure
    - Strength Reduction Factor for Concrete
- α = .80 Accounts for unintended eccentricity or bending moment
    - Strength Reduction Factor for Concrete

To calculate the appropriate area of concrete and area of steel the United States Standard Bar size chart was consulted for dimensions. For the purpose of this study, four #9 bars were used. As can be seen in Figure 36, the area of a #9 bar is 1.00 in^2. The column capacity was calculated for columns having four and six bars. A computer program called the *Design and Analysis of Reinforced Concrete Column Calculator* was used as a check against the values obtained using Equation 10. This calculator was developed by Jonathan Ochshorn who is a professor at Cornell University. Following the check, all values were input into a spreadsheet to compare with the values obtained for capacity loss.

Table 7-1.—U.S. Standard Reinforcing Bars

U.S. Standard Reinforcing Steel Bars				
Bar Size Designation	Area Square Inches	Weight lb Per Foot	Diameter	
			inches	mm
#3	.11	.376	.375	9.53
#4	.20	.668	.500	12.7
#5	.31	1.043	.625	15.88
#6	.44	1.502	.750	19.05
#7	.60	2.044	.875	22.23
#8	.79	2.670	1.000	25.40
#9	1.00	3.400	1.128	28.58
#10	1.27	4.303	1.270	31.75
#11	1.56	5.313	1.410	34.93
#14	2.25	7.650	1.693	43.00
#18	4.00	13.600	2.257	57.33

Figure 36: Standard Reinforcing Bar Sizes [48]

B.1.9 Calculations

To reiterate the NSC and HSC columns designed, Table 4 was created. It was given in the results section and is repeated here for convenience.

Table 3: Design Parameters for NSC and HSC at ambient temperatures [22]

	NSC	HSC
Size	20in. by 20in.	20in. by 20in.
Compressive Strength	35MPa (5,000psi)	110MPa (16,000psi)
Tensile Strength	2MPa (283psi)	3.5MPa (506psi)
Yield Strength	414MPa (60,000psi)	414 MPa (60,000psi)
W/C	0.48	0.30
Cement Type	Portland Cement Type I	Portland Cement Type I
Aggregate Size	19mm (0.75in.)	19mm (0.75in.)
Steel Reinforcements	Deformed Steel	Deformed Steel
Admixtures	None	None
Cover	38mm (1.5in.)	38mm (1.5in.)
Reinforcements	4 #9 bars	4 #9 bars

To calculate capacity:

1.) Choose a Steel Reinforcement From Figure 36 and Check Reinforcement Ratio

Four #9 Bars

$$Pg = \frac{(4\ bars * 1.00in^2)}{(20\ in^2 * 20\ in^2)} = 1\%\ \checkmark$$

2.) Convert $f'c$ to ksi (kips per square inch) for simplicity

$$f'c = 5{,}000\ psi\ \left(\frac{1\ ksi}{1{,}000\ psi}\right) = 5\ ksi$$

3.) Convert fy to ksi for simplicity

$$fy = 60{,}000\ psi\ \left(\frac{1\ ksi}{1{,}000\ psi}\right) = 60\ ksi$$

4.) Calculate Area of Steel

$Ast = (4\ bars * 1.00in^2) = 4\ in^2$ (Area of #9 bar is$1.00in^2$)

5.) Calculate Area of the Concrete Cross Section

$$Aconc = (20\ in. * 20\ in.) - (4\ bars * 1.00in^2) = 396\ in^2$$

6.) Calculate Capacity Using Equation 10

$$Pn = [.85(5\ ksi)(396\ in^2) + (60\ ksi)(4\ in^2)](.65)(.80) = \boxed{1000\ kips}$$

Repeat the Process for HSC with Different Reinforcement (Demonstration Purposes):

1.) Choose a Steel Reinforcement From Figure 36 and Check Reinforcement Ratio

Six #18 Bars

$$Pg = \frac{(6\ bars * 4.00in^2)}{(20\ in^2 * 20\ in^2)} = 6\%\ \checkmark$$

2.) Convert $f'c$ to ksi (kips per square inch) for simplicity

$$f'c = 16{,}000\ psi\ \left(\frac{1\ ksi}{1{,}000\ psi}\right) = 16\ ksi$$

3.) Convert fy to ksi for simplicity

$$fy = 60{,}000\ psi\ \left(\frac{1\ ksi}{1{,}000\ psi}\right) = 60\ ksi$$

4.) Calculate Area of Steel

$Ast = (6\ bars * 4.00in^2) = 24\ in^2$ (Area of #18 bar is$4.00in^2$)

5.) Calculate Area of the Concrete Cross Section

$Aconc = (20\ in. * 20\ in.) - (6\ bars * 4.00in^2) = 376\ in^2$

6.) Calculate Capacity Using Equation 10

$Pn = [.85(16\ ksi)(376\ in^2) + (60\ ksi)(24\ in^2)](.65)(.80) =$ $\boxed{3408\ kips}$

The capacity equation remains the same when determining the capacity during a spall. For a 10 mm, 20 mm, 30 mm, or 40 mm spall the same equation is used, however the $Aconc$ reduces because of the cross sectional loss.

Ex. 20 mm loss: $Ag = (20\ in. - .79\ in.) * (20\ in. - .79\ in.) = 369\ in^2$

The yield strength and compressive strength also reduce when in a fire environment. The process to obtain those values is displayed in Appendix C. Those values can then be input into this equation with the cross sectional loss values to determine a new capacity. Comparing this capacity against the original capacity gives a percentage of capacity lost.

Appendix C

C.1 Strengths at Elevated Temperature

The fundamental equation that predicts spalling (Equation 1) relies on the decreasing tensile strength of the concrete as temperature increases. The capacity equation for reinforced concrete columns (Equation 10) relies on the decreasing compressive strength of the concrete and yield strength of the reinforcing steel as temperature increases. The tensile and compressive strengths of concrete, and the yield strength of steel, decrease at elevated temperatures. The methods and approximation of these values are described herein.

C.1.1 Tensile Strength of Concrete

Kodur 's "Hydrothermal Model for Predicting Fire-Induced Spalling in Concrete Structural Systems" predicts the tensile strength as the temperature increases (Equation 2). Table 2 displays example data of the tensile strength of the NSC and HSC columns as temperature increases.

Equation 11: Tensile strength as a function of temperature [38]

$$f_{tT} = \begin{cases} f_t, & T \leqslant 100\,^{\circ}\mathrm{C} \\ f_t \frac{600-T}{500}, & 100\,^{\circ}\mathrm{C} < T \leqslant 550\,^{\circ}\mathrm{C} \\ f_t \frac{1200-T}{6500}, & 550\,^{\circ}\mathrm{C} < T \leqslant 1200\,^{\circ}\mathrm{C} \\ 0, & T > 1200\,^{\circ}\mathrm{C} \end{cases}$$

C.1.2 Compressive Strength of Concrete

The compressive strength of the concrete decreases at elevated temperatures according to Equation 3, from "*Eurocode 2*" [2]. Table 2 displays example data of the compressive strength of the NSC and HSC columns as temperature increases.

Equation 12: Compressive strength as temperature increases [37]

$$f'_{cT} = \begin{cases} f'_c & T \leq 100\text{°C} \\ f'_c(1.067 - 0.00067T) & 100\text{°C} \leq T \leq 400\text{°C} \\ f'_c(1.44 - 0.0016T) & T \geq 400\text{°C} \end{cases}$$

C.1.3 Yield Strength of Steel

The change of yield strength over temperature has been tested and documented through Topcu and Karakirt's "Properties of Reinforced Concrete Steel Rebars Exposed to High Temperatures" research (see Figure 20- S420 steel was used for this study). Table 4 displays example data of the yield strength of the reinforcing steel as temperature increases.

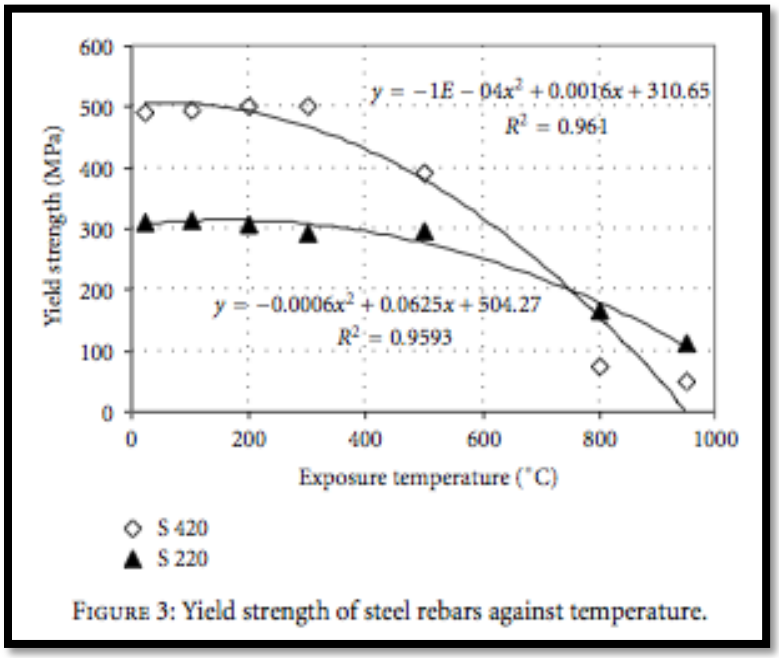

Figure 37: Loss of Yield Strength over Temperature [41]

Table 4: Concrete and Reinforcing Steel Strength Decreases at Elevated Temperatures

Temperature (deg C)	NSC (MPa)		HSC (MPa)		Reinforcing Steel
	Tensile	Compressive	Tensile	Compressive	Yield (MPa)
100	283	34	506	110	507
200	226	32	405	103	493
300	170	30	304	95	464
400	113	28	202	88	429
500	57	22	101	70	379
600	26	17	47	53	314
700	22	11	39	35	236
800	17	6	31	18	150
900	13	0	23	0	54

Appendix D

D.1 Spalling Prediction Inequality

To predict spalling the fundamental equation for pore pressure given by Kodur is given as follows: ($P_v > \frac{f_t'}{n}$). A spalling prediction is made if the pore pressure value exceeds the tensile strength of the concrete divided by the porosity. The points at which a spall occurs can be seen in graphs as shown in Figure 27.

D.1.1 Pore Pressure

Pore Pressure (P_v) is the most important factor of this study. Pore pressure values are shown in Figure 23 and are based off of Kodur's data. The intersection points between these values and the tensile strength divided by the porosity values indicate a spall has occurred.

D.1.2 Tensile Strength

The tensile strength used for this inequality was the same as described in Section C.1.1 Tensile Strength of Concrete.

D.1.3 Porosity

Porosity values were obtained from Hernandez porosity equation based on water-cement ratio [35]. For example, the W/C used for the NSC in this study was .48. The porosities given by Hernandez are shown here in Table 5.

Table 5: Porosity as a function of W/C [35]

W/C	Porosity (%)
.45	15.93
.50	18.04
.55	19.94
.60	20.81

To obtain the porosity value for a W/C value of .48 linear interpolations were used as shown here:

$$\frac{.50 - .45}{18.04 - 15.93} = \frac{.50 - .48}{18.04 - x} \qquad porosity = x = 17.2\%$$

Appendix E

E.1 Supplemental Figures

The figures included in this Appendix supplement those presented in the Methodology and Results sections. They were left out of these sections to avoid redundancy.

E.1.1 Temperature vs. Pore Pressure

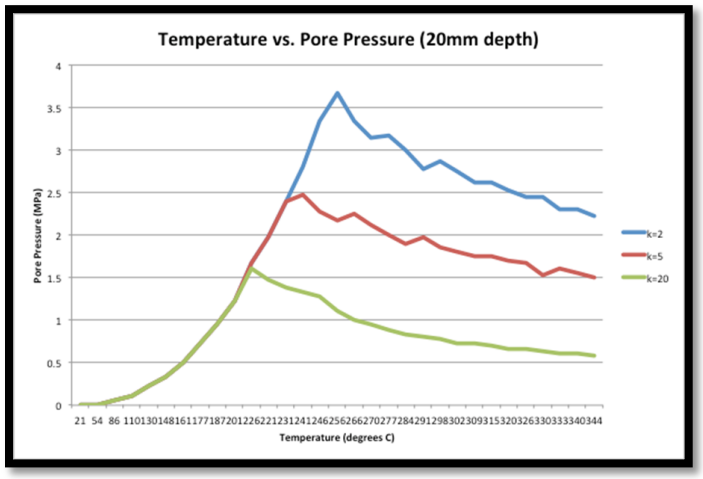

Figure 38: Temperature vs. Pore Pressure @ 20mm Depth

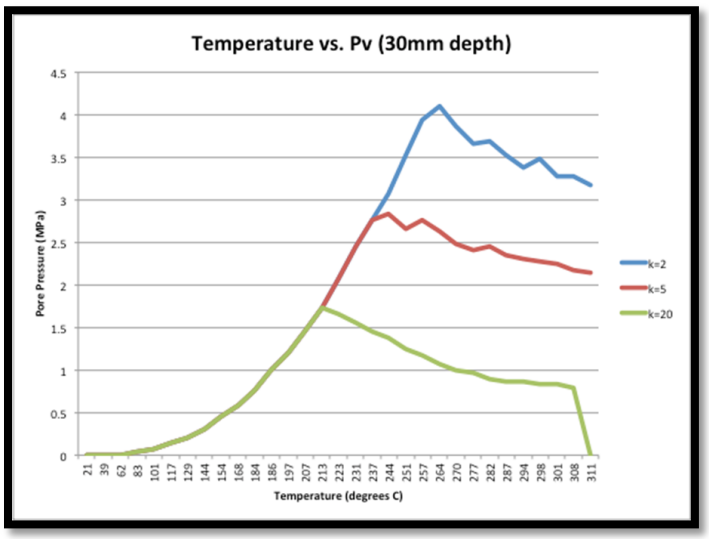

Figure 39: Temperature vs. Pore Pressure @ 30mm Depth

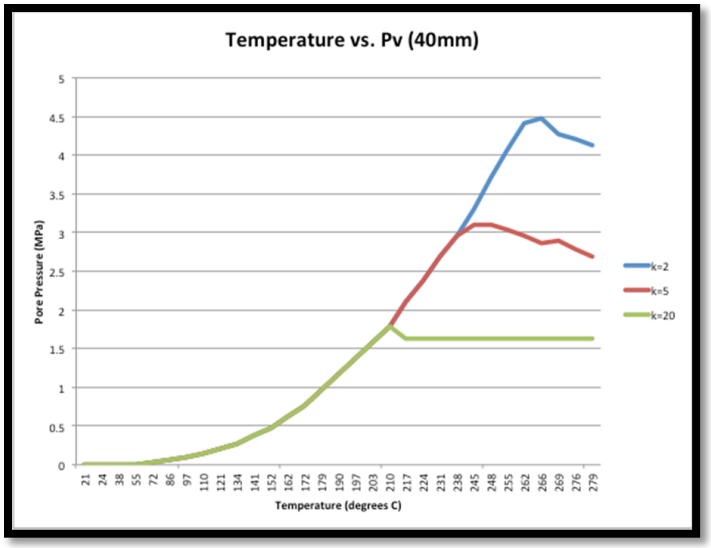

Figure 40: Temperature vs. Pore Pressure @ 40mm Depth

E.1.2 Temperature of Furnace versus Temperature @ Specified Depth

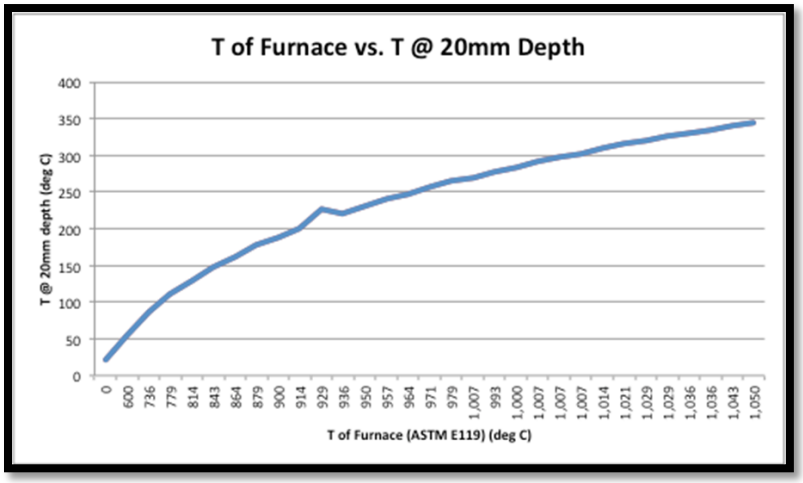

Figure 41: Temperature of Furnace *(ASTM E119)* vs. Temperature @ 20mm Depth

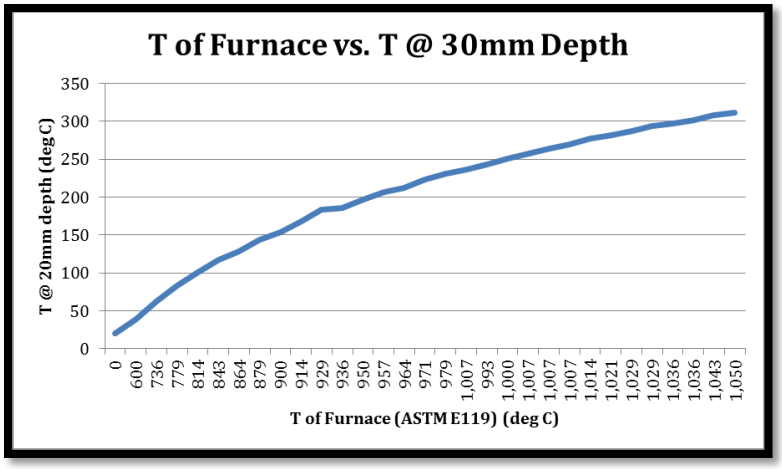

Figure 42: Temperature of Furnace *(ASTM E119)* vs. Temperature @ 30mm Depth

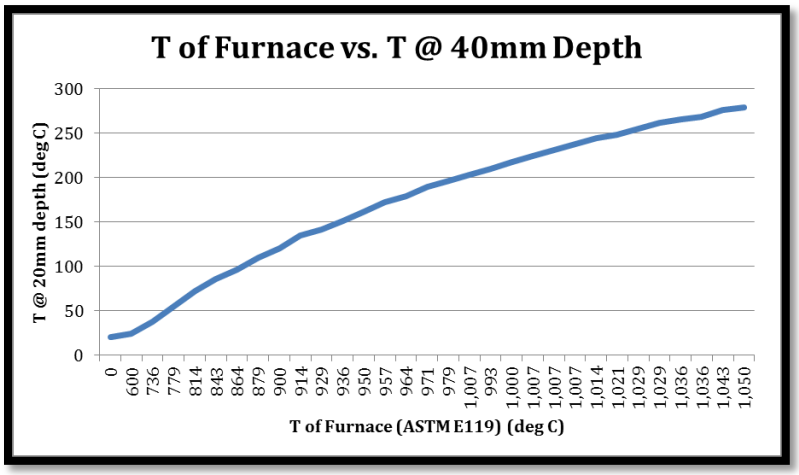

Figure 43: Temperature of Furnace (*ASTM E119*) vs. Temperature @ 40mm Depth

E.1.2.3 Temperature versus Total Capacity Loss of NSC

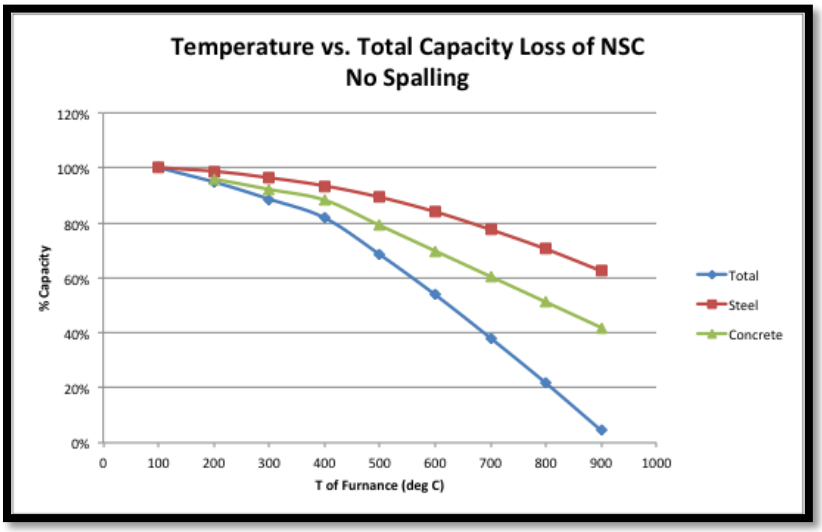

Figure 44: Temperature vs. Total Capacity of NSC (No Spalling)

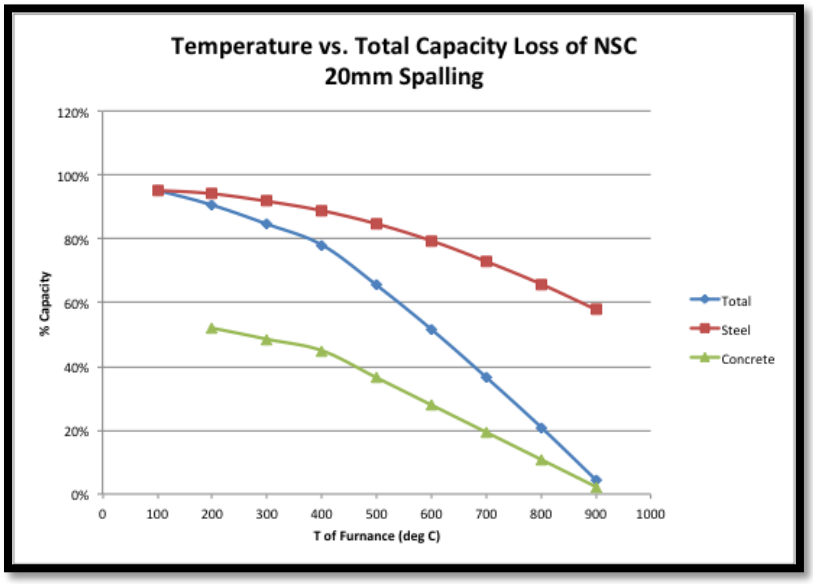

Figure 45: Temperature vs. Total Capacity of NSC (20mm Spalling)

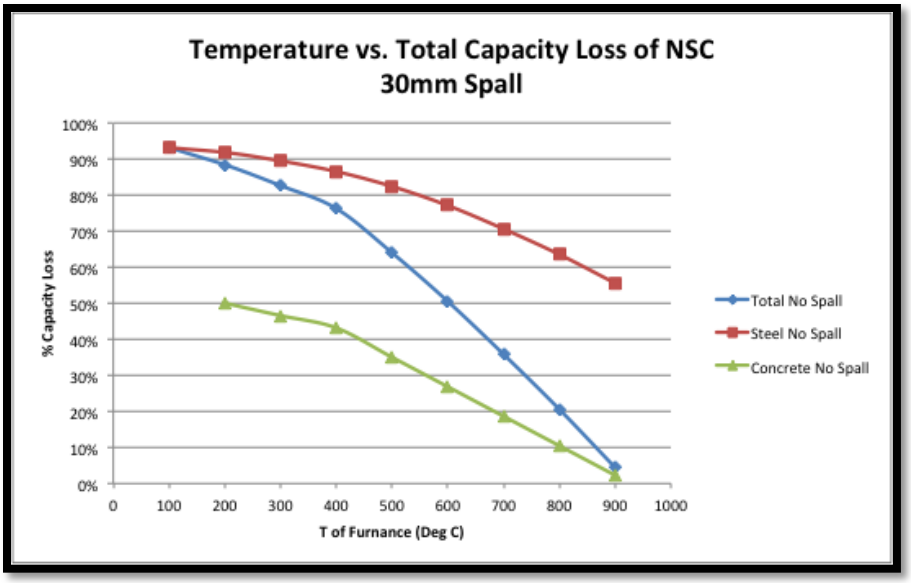

Figure 46: Temperature vs. Total Capacity of NSC (30mm Spalling)

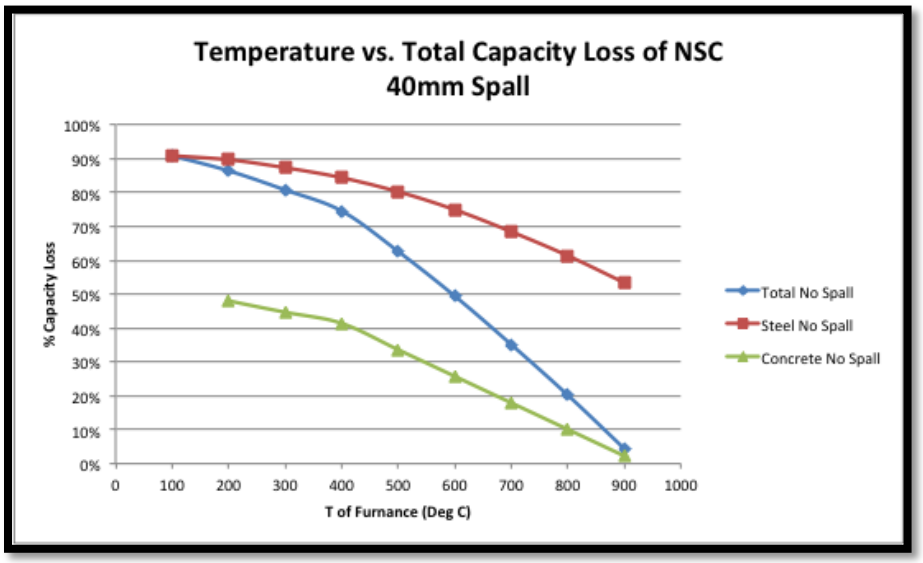

Figure 47: Temperature vs. Total Capacity of NSC (40mm Spalling)